



Faunal behavior in response to near bottom water dynamics in a marine protected area (Cantabrian Sea, southern Bay of Biscay)

Francisco Sánchez^a, Cesar González-Pola^b, Augusto Rodríguez-Basalo^a,
Juan Manuel Rodríguez^a, Elena Prado^a, Larissa Módica^a, Cristina Rodríguez-Cabello^{a,*}

^a IEO, Promontorio San Martín s/n., 39004, Santander, Spain

^b IEO, Avda. Príncipe de Asturias, 70 bis, 33212, Gijón, Spain

ARTICLE INFO

Keywords:

Lander
Deep-sea biodiversity
Oceanographic dynamics
Fish behavior
El cachucho MPA
Le Danois bank

ABSTRACT

A set of lander deployments in a deep marine protected area (MPA; El Cachucho) combining environmental sensors and a baited camera provided insight on the relationship between faunal behavior and oceanographic dynamics. Landers were deployed at different depths, ranging from 500 to 960 m for a period of 24–26 h. A total of 10,989 photographs were downloaded and synchronized using a time code with all the environmental variables recorded (pressure, temperature, salinity, water current, and direction). Total richness accounted for 41 species of different taxonomic groups (21 fishes, 11 crustaceans, 6 echinoderms, and 3 molluscs). The most abundant species were *Synphobranchius kaupii*, *Mora moro*, *Phycis blennoides*, *Helicolenus dactylopterus*, and *Etmopterus spinax*. Arrival times (T_{arr}) and maximum number of individuals (N_{max}) greatly differed among stations.

Cluster analysis showed two main faunal groups in relation to depth: those close to the top of the bank and those in the flanks. Species densities were estimated using Priede's equations and compared with those obtained in previous studies using trawl samplers. The relation of species with environmental variables showed high variability depending on the location of the station and the associated variables (depth, current, and water masses). Near-bottom dynamics were consistent with previously known oceanographic patterns at the bank, dominated by background anticyclonic recirculation along the flanks overlaid by strong tidal cycles. Current and hydrography tidally driven phases showed an evident effect in the arrival of species at some locations. Species appeared during specific periods matching the beginning of the flooding phase or end of the ebb phase. Movement rates (cm s^{-1}) were estimated for some invertebrate species, such as crabs (*Bathynectes maravigna*, 0.66; *Pagurus* sp., 0.09), the gasteropod *Colus gracilis* (0.15), and echinoderms (*Cidaris cidaris*, 0.04; *Araeosoma fenestratum*, 0.23).

1. Introduction

The use of noninvasive methods is becoming crucial in the study of singular habitats or vulnerable species. Baited cameras or in general terms baited remote underwater video stations (BRUVS) have become a widely used technique for assessing patterns of animal behavior, abundance and biodiversity. The benefits of this technique—namely, its nondestructive and nonextractive nature, its easy replication, and its relatively low cost compare to other techniques—are well documented (Priede and Bagley, 2000; Bailey et al., 2007; Cappel et al., 2007).

Le Danois Bank (Le Danois, 1948), locally named *El Cachucho* fishing ground, is a marginal shelf—a seamount-like topographic feature nearby and partially connected to the continental shelf—located in the central Cantabrian Sea (Bay of Biscay, NE Atlantic) at a distance of 65 km from the northern coast of Spain. Several research surveys were conducted in this area from 2003 to 2009 under the ECOMARG project. The high biodiversity found in this area (Sánchez et al., 2008; Altuna, 2013) and the presence of endangered species and vulnerable habitats (coral reefs) engendered its protection (Rodríguez-Basalo et al., 2019).

In 2008, El Cachucho was declared the first large off-shore marine

* Corresponding author.

E-mail addresses: francisco.sanchez@ieo.csic.es (F. Sánchez), cesar.pola@ieo.csic.es (C. González-Pola), augusto.rodriguez@ieo.csic.es (A. Rodríguez-Basalo), juanmanuel.rodriguez@ieo.csic.es (J.M. Rodríguez), elena.prado@ieo.csic.es (E. Prado), larissa.modica@ieo.csic.es (L. Módica), cristina.cabello@ieo.csic.es (C. Rodríguez-Cabello).

<https://doi.org/10.1016/j.ecss.2022.108078>

Received 29 December 2021; Received in revised form 31 August 2022; Accepted 14 September 2022

Available online 22 September 2022

0272-7714/© 2022 The Authors. Published by Elsevier Ltd. This is an open access article under the CC BY-NC-ND license (<http://creativecommons.org/licenses/by-nc-nd/4.0/>).

protected area (MPA) in Spain by the Spanish Ministry of Environment (Heredia et al., 2008) and was included in the Natura 2000 network in the category of special area of conservation (SAC) following the principles established by the European Union (EU). Since then, the consequences of the management measures applied in MPAs must be scientifically monitored, and noninvasive methods, such as acoustic and visual surveys, must be used for their assessment and monitoring of MPAs.

The main reason for the inclusion of El Cachucho in the Natura 2000 network was the presence of reefs (habitat 1170 of the Habitats Directive; EU, 2002). To study these vulnerable habitats and their conservation status, visual transects using a photogrammetric sled and remote operate vehicles (ROVs) have been used in previous research (Sánchez et al., 2017). However in order to improve the knowledge and monitoring system of this area, oceanographic dynamics near the seafloor and mobile fauna have also been recently studied by deploying an anchored multiparametric observatory (lander). Additionally lander deployments allow to record environmental variables in a large temporal scale. Results of this new approach are presented in this study.

Estimates of species abundance, although fundamental to marine ecology, are difficult to obtain under certain circumstances that preclude the intensive use of trawl sampling or other extractive sampling gears (Farnsworth et al., 2007). The use of ROVs and photogrammetric sleds is necessary to investigate the conservation status of benthic habitats. However, these provide poor information about the mobile species that live in these habitats. Within this framework, baited cameras and landers—multiparametric benthic platforms—represent an important alternative tool for the study and monitoring of MPAs. It is necessary to assess whether these approaches provide valuable information and can be used as additional techniques to detect changes in space and time. Our study provides, for the first time, information on mobile organisms attracted to baited cameras and their relationship with environmental variables observed near the sea floor.

The main purpose of the present work is to determine whether faunal behavior in the deep ocean is related to local short-term oceanographic dynamics, in particular, to tidal cycles in the study area. Our goals are (1) to investigate the near-bottom oceanographic dynamics at specific sites in the MPA, (2) to estimate the abundance and distribution of the fauna attracted to the bait, (3) to study the behavior of benthic species in relation to oceanographic variables, and (4) to estimate the mobility of some benthic invertebrates.

2. Materials and methods

2.1. Study area

The present study is based on data collected from several sampling stations located in the central Cantabrian Sea (the southern Bay of Biscay) using a multiparametric benthic platforms (landers). These platforms were submerged at different positions on the sea floor in the El Cachucho MPA, which comprises Le Danois Bank and its intraslope basin.

The bank presents an elongated E–W disposition, with depths on the plateau summit ranging between 450 and 600 m (Fig. 1). The northern face shows a pronounced slope from 500 m at the top of the bank to more than 4000 m on the abyssal plain, which lies only 9 km to the north (Sánchez et al., 2008).

The bank is partially connected to the continental shelf through an intraslope basin; thus, its dynamics are affected either by the general background circulation of the Bay of Biscay or the slope current development. Eastern North Atlantic Central Water (ENACW, e.g., van Aken, 2001) fills the upper Bay of Biscay, flowing as an anticyclonic loop with a weak southward component of $\sim 1 \text{ cm s}^{-1}$ (Pingree, 1993; van Aken, 2002). A salinity minimum is reached at a depth of 450–500 m, starting the transition towards the Mediterranean outflow waters with its core at $\sim 1000 \text{ m}$ (van Aken, 2000). The upper slope is affected by the entrance of the Iberian Poleward Current (IPC) in the Cantabrian Sea during the autumn–winter period (Pingree and Le Cann, 1990) and the advance of much deeper Mediterranean outflow water (MOW) along the western European margin (Iorga and Lozier, 1999).

The circulation dynamics at Le Danois have been extensively studied in the framework of the projects that motivated the declaration of the area as an MPA (González-Pola et al., 2012). Records show a stable anticyclonic flow at the seamount summit, especially in the western side, characterized by a rocky outcrop. Such flow seems to be supported by a combination of the temporary formation of Taylor cap and the rectification of the strong semidiurnal tide. Geomorphological studies in the region have provided a detailed analysis of the bedforms in relationship with the circulation (van Rooij et al., 2010; Hernández-Molina et al., 2016). Bottom currents are locally accelerated (up to 25 cm s^{-1}) due to the presence of the Le Danois Bank and the Vizco High, creating a furrow and moats of high importance in the area in terms of sediment transport of the contourite system (Liu et al., 2019). On the southern flank of the Bank and north of the slope of Cantabrian Sea continental

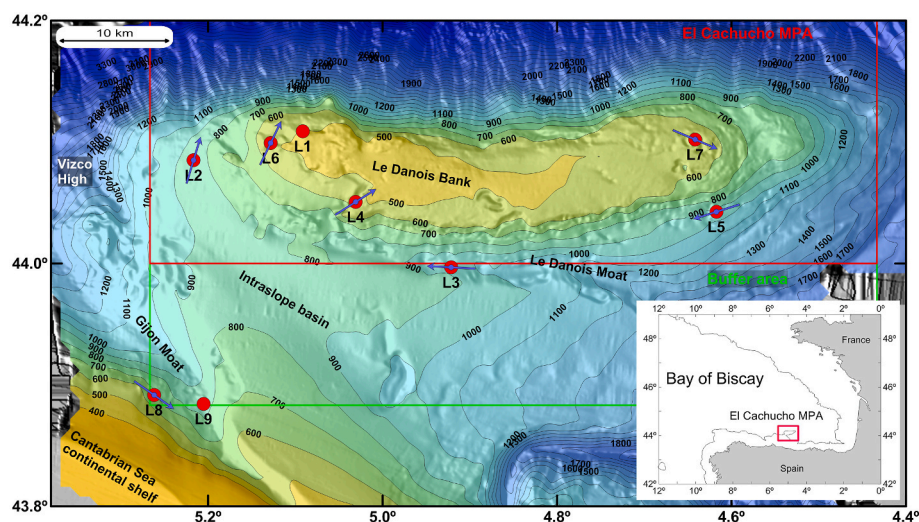


Fig. 1. Study area and lander deployments on El Cachucho MPA (Le Danois Bank). Red and green lines show the areas with specific management measures. Blue arrows over lander locations indicate along-slope direction, based on local high-resolution topography, on which currents were then projected. (For interpretation of the references to colour in this figure legend, the reader is referred to the Web version of this article.)

shelf there are two channels, the Le Danois Moat and Gijón Moat respectively (Fig. 1).

To study the monitoring of the MPA El Cachucho, surveys were conducted on board of the research vessels (RVs) Angeles Alvariño and Ramón Margalef in July 2009, May 2014, and July 2019. Nine lander deployments were conducted at different sites. To cover the whole tidal phases, the lander was deployed for at least 24 h in almost every station. The lander payload varied slightly due to equipment availability and technical reasons.

Lander deployments are described in Table 1 and Fig. 1. Four deployments were conducted at the top of the bank at depths ranging from 500 to 650 m, three in the southern flank at depths ranging from 850 to 960 m, and two in the southwest area between the continental shelf and the intraslope basin at depths ranging from 678 to 841 m. For lander deployments 1 and 9, a current meter was not available; therefore, these landers cannot be used to infer patterns between communities and oceanographic conditions. Landers 2, 5, 6, and 7 were located along the bank flanks where the along-slope anticyclonic circulation is anticipated, and landers 3, 4, and 8 were located in specific canyon-like topographic features, so expected dynamics are related to the local tide-topography interaction. A fine scale topography view of deployment sites can be found for selected landers in Section 3.

2.2. Sampling device: lander

A lander system designed to obtain high frequency bottom photography and environmental variables was equipped for deployment at strategic locations in the study area. The system consisted of a ballasted tripod made of stainless steel holding an underwater camera, baits, and several sensors. The lander was designed at the oceanographic center of Santander (Spanish Oceanographic Institute: IEO) by members of the ECOMARG research team (Sánchez et al., 2014; www.ecomarg.com) and incorporates several different sensors to study the near-bottom environmental conditions together with lapse-time images (Fig. 2). The structure was deployed and recovered using a main rope with buoyancy elements attached.

The environmental basic payload present in landers 2 to 8 included an Aquadopp single-point current meter with temperature and pressure sensors sampling at 1-min intervals to record near-bottom (c.a. 2 mab; meters above bottom) conditions. An upward looking Acoustic Doppler

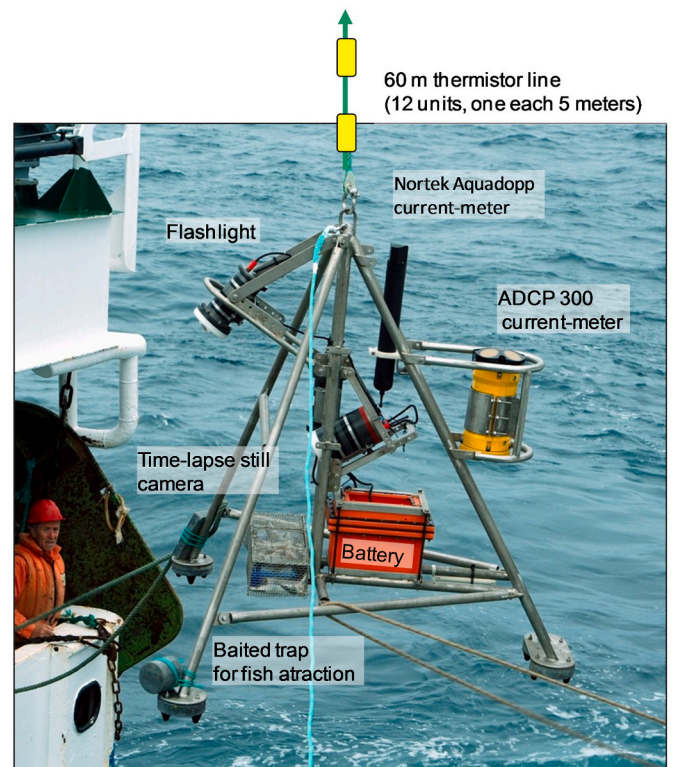


Fig. 2. Lander system design and equipment.

Current Profiler (ADCP) RDI Sentinel-300 recording the vertical structure of the currents up to 80 mab was also included and additionally, in landers 2 to 5, a thermistor chain containing 12 Sbe56 thermometers spaced at 5-m intervals above the lander (measuring up to 57 mab) and programmed at 1 Hz was installed. A SeaBird37 CTD recording at 10-s intervals was placed at the top of the thermistor chain if present or at the lander otherwise. For the purpose of this study we focus on the single-point current meter record and refer indirectly to ADCP and thermistor chain information intended to describe local mixing

Table 1

Summary and characteristics of each deployment. Mean and (±) standard deviation values for the environmental variables are indicated. The range, minimum and maximum values are specified in brackets.

	Lander 1	Lander 2	Lander 3	Lander 4	Lander 5	Lander 6	Lander 7	Lander 8	Lander 9
Longitude	005°05.482'W	005°13.000'W	004°55.283'W	005°01.849'W	004°37.039'W	5°07.699'W	4°38.500'W	5°15.710'W	5°12.310'W
Latitude	44°06.536'N	44°05.099'N	43°59.808'N	44°03.040'N	44°02.552'N	44°05.950'N	44°06.127'N	43°53.500'N	43°53.064'N
Date (dd/mm/yyyy)	31/05/2014	08/06/2014	10/06/2014	12/06/2014	15/06/2014	19/07/2019	21/07/2019	24/07/2019	24/07/2009
On the bottom (hh:mm)	7:49	16:19	12:27	16:28	6:56	6:44	7:20:13	7:57:58	17:26:06
Duration (hh:mm)	33:20:00	26:10:00	23:31	21:49	23:42	31:14:00	26:28:00	28:41:00	21:20:00
Photo time lapse	0:02:00	0:02:00	0:01:30	0:01:30	0:01:30	0:01:00	0:01:00	0:01:00	0:01:00
Number photos	1001	786	942	874	949	1874	1588	1701	1274
Depth (m)	498	886	955	641	945	537	551	678	841
Temperature (°C)	11.11 ± 0.08	10.26 ± 0.05	10.05 ± 0.09	10.96 ± 0.05	10.02 ± 0.06	10.92 ± 0.04	10.93 ± 0.02	10.55 ± 0.05	10.40 ± 0.056
Temperature range	(10.97–11.27)	(10.16–10.35)	(9.80–10.17)	(10.89–11.12)	(9.90–10.15)	(10.80–11.03)	(10.88–10.95)	(10.47–10.70)	(10.34–10.51)
Salinity (ppm)	35.64 ± 0.01	35.74 ± 0.01	35.75 ± 0.01	35.61 ± 0.01	35.75 ± 0.01	35.58 ± 0.01	35.57 ± 0.01	35.69 ± 0.02	35.81 ± 0.03
Salinity range	(35.58–35.74)	(35.72–35.76)	(35.71–35.77)	(35.55–35.69)	(35.68–35.78)	(35.10–35.63)	(35.52–35.60)	(35.63–35.70)	(35.75–35.83)
Current speed (cm/s)	–	7.61 ± 2.80	6.10 ± 2.70	9.10 ± 3.00	11.05 ± 4.70	7.30 ± 3.60	6.60 ± 3.40	12.30 ± 6.10	–
Max current speed (cm/s)	–	14.80	13.20	22.30	21.40	21.40	15.40	33.20	–

processes.

A camera Nikon D80 with a 20-mm focal lens was placed inside an underwater capsule, which took pictures at 2- or 1.5-min intervals. The camera was located 1.6 m above the sea floor with an angle of 35°. Image resolution was 12 Mp, and field of view covered by the flash light illumination was approximately 3.5 m² (Fig. 3). Additionally, the lander system incorporates a subtrobe Subtronic Mega with 250 Ws power and auxiliary elements, such as a battery DSPL, junction box, wires, and a bait holder (Fig. 2).

Species were attracted using bait. The bait holder was filled with a consistent quantity (~3 kg) of frozen mackerel (*Scomber scombrus*) and horse mackerel (*Trachurus trachurus*), chopped to maximize the odor plume. To preserve the bait for a longer time and avoid quick consumption by earliest scavengers or predators, the bait was placed inside a metallic grid basket (Fig. 2). The objective was to keep the attraction to fish and other benthic organisms during the whole mooring period.

As a common procedure to analyze the environmental conditions time series together with images, we project the measured currents onto the local isobaths direction. For the landers located along the flanks of the bank, we defined as positive the along-isobath circulation describing the aforementioned anticyclonic loop as well as the cross-isobaths to the right (from deeper to shallower). For landers in canyons, moats, or incisions we defined as positive the along-isobath direction—axis of the feature—towards its head (shallower) and the cross-isobath direction to the right. The convention is shown by arrows in Fig. 1. Topographic details of lander deployment sites are shown in Fig. 4.

2.3. Image analysis

Images were downloaded and synchronized using a time code with all the environmental variables recorded by the sensors. The camera resolution (12 Mp) was sufficient to identify all species larger than approximately 2 cm total length (Fig. 3). All species were identified to the lowest taxon possible. The identification was based on expertise knowledge and previous sampling conducted in the area before the establishment of the MPA (Sánchez et al., 2008; 2009, 2017). Owing to the difficulties associated with species identification based on images, we followed the open taxonomic nomenclature for image-based identification (Horton et al., 2021). Due to their small size, amphipods and isopods were not counted individually; however, an estimation of the numbers observed in each lander deployment was assessed according to

the following scale: 0: not observed; 1: less than 10 individuals; 2: from 11 to 50; and 3: more than 50. Thus, an approximation of the species abundance observed in each lander was obtained. For each image, time (t), species identified, and maximum number of individuals of a given species (N_{\max}) were recorded. The first arrival time (t_{arr}) was determined by the minutes elapsed from the lander arrival at the sea floor to the first individual appearance within the field of view of the camera. These data were combined with environmental data obtained from sensors (pressure, temperature, tide period, etc.).

2.4. Statistical analysis

We analyzed species contribution to similarity of each deployment. Multivariate analysis was conducted with PRIMER 5 (Clarke and Warwick, 2001) based on species peak abundance N_{\max} , using the square root transformation to reduce the influence of dominant species.

A similarity matrix was created using the Bray–Curtis index, and a cluster analysis was performed to obtain sample dendrograms. A similarity of percentages analysis (SIMPER) was performed to estimate the percentage contribution of each species to intragroup similarity (Clarke and Warwick, 2001).

To estimate species density, we followed the methodology by Priede and Merrett (1996). Time of first arrival (t_{arr}), species speed (V_f), and current speed (V_w) were used to estimate the radius (r) of the space occupied by each fish using the following equation:

$$r = \frac{t_{\text{arr}}}{\left(\frac{1}{V_f} + \frac{1}{V_w}\right)}$$

According to these authors, $V_f = V_w = 0.05 \text{ m s}^{-1}$ is assumed to be typical of deep ocean conditions. Nevertheless, in the present study, V_w values were obtained from direct measurements recorded from each lander station (Table 1). V_f estimates of some fish and invertebrates obtained in the present study were also applied (Section 2.5.). The theoretical fish population density (A) expressed as the number of fish per Km² was calculated using the following equation (Priede and Merrett, 1996):

$$A = \frac{10^6}{3r^2}$$

In the present study, we included information on biological traits (BT) for all species identified to determine the potential usefulness of

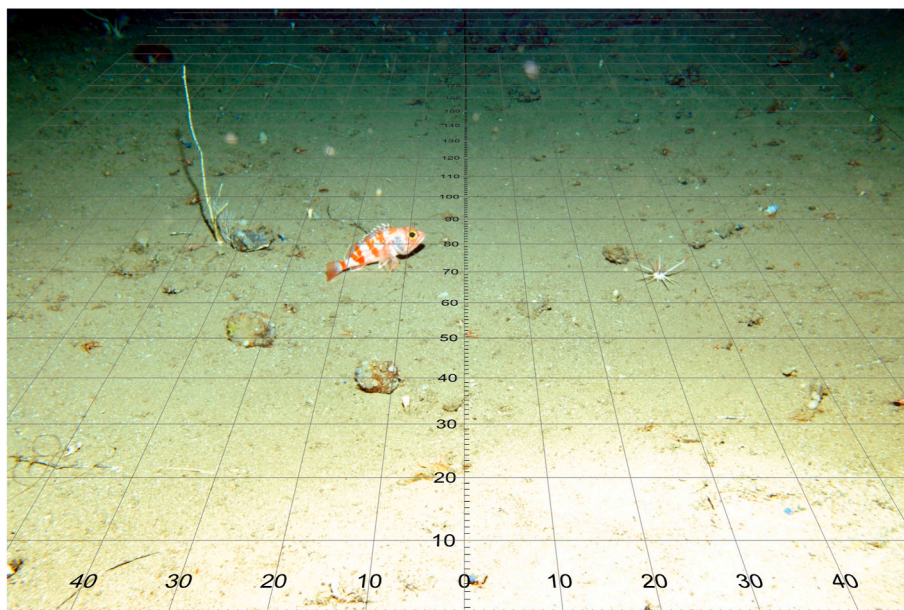


Fig. 3. Image scaling and method used to estimate track distance for some benthic species.

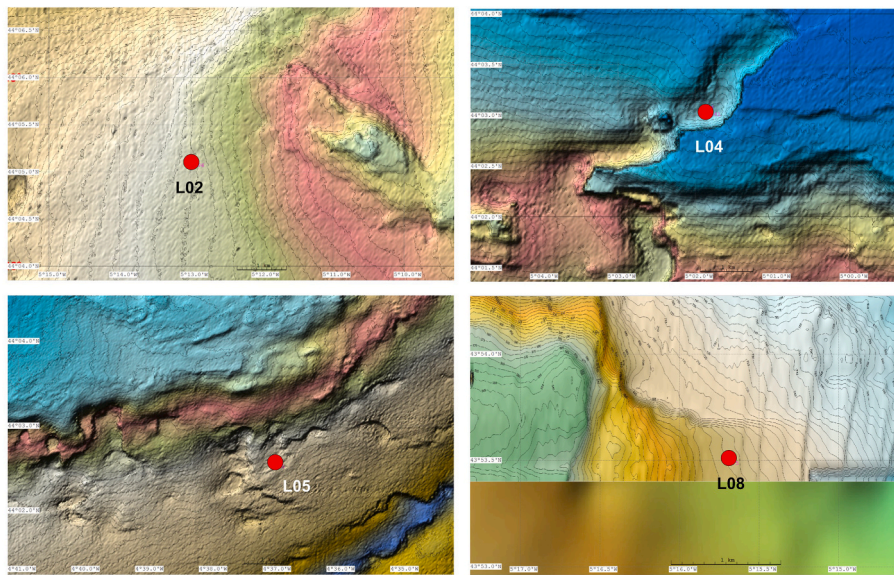


Fig. 4. Detail topography of landers 2, 4, 5, and 8.

landers in the study of deep-sea species behavior in comparison with other marine ecosystems. BT variables considered as good characterizations of species living in these habitats in relation to the sampling methodology were relative size (*S*), relative mobility (*M*), adult movement (*V*), and feeding habits (*E*).

Table 2 presents the different categories of each BT variable. Information was collected from literature and the main databases available: Fishbase (Froese and Pauly, 2019), Sealife (Palomares and Pauly, 2020), WoRMS Editorial Board (2021), and the biological traits information catalogue (BIOTIC) (MarLIN, 2006). We used the cumulative BT scores of each variable as a BT index to select species in relation to habitat characterization (Sánchez et al., 2017; Bremner et al., 2006).

2.5. Mobility analysis

The estimation of velocity and movement patterns of some of the invertebrate species observed during lander deployments included the steps:

1. Selection of frames with representative species (large benthic invertebrates frequently observed)

Table 2

Biological trait variables and categories used to describe ecological functioning of species in the study area based on the information recorded in each lander deployment.

Biological trait variables	Code	Category	
Relative size (<i>S</i>)	1	Small	<2 cm
	2	Small-medium	2–10 cm
	3	Medium	10–30 cm
	4	Medium-large	30–80 cm
	5	Large	>80 cm
Relative mobility (<i>M</i>)	1	None	
	2	Low	
	3	Medium	
	4	High	
Adult movement (<i>V</i>)	1	Sessile	
	2	Burrow	
	3	Crawl	
	4	Swim	
Feeding habit (<i>E</i>)	1	Deposit	
	2	Filter/suspension	
	3	Predator	
	4	Opportunist/scavenger	

2. Georeference and scaling the selected images (Fig. 3)
3. Detect changes (differences among images) focusing on target species
4. Measure distance between consecutive positions
5. Calculate velocity using time lapse between images

The track done by target species has a geographical reference (WGS84 UTM-30N), allowing for the measurement of distances in the image. All processing was performed using QGIS (v.3.16) software.

3. Results

3.1. Environmental dynamics

Currents recorded in all landers can be seen as direction, frequency, and strength “Current rose” compositions on Fig. 5. This figure represents a collection of snapshots where full raw records are represented—not accounting exactly for equivalent complete tidal cycles—and spring–neap tidal cycles also differ among landers. Figs. 6 and 7 provide time series of hydrographic and current records together with lapse-time photography results for selected landers. Time series of the remaining landers are shown in Supplementary Figs.

Overall, current records agree well with our previous knowledge of the bank and canyon-like features general functioning. Deployments 2, 3 and 5 were located along the flanks of the bank, where anticyclonic (AC) recirculation is expected. Deployments 6 and 7 (located W and NE of the top of the bank, respectively) were those that most clearly followed this AC pattern for the overall tidal cycle without large reversals (i.e., NW and SE flow, respectively, in agreement with isobath alignment depicted in Fig. 1). Lander 2 time series details (Fig. 6A) show a single along-slope flow reversal around the mid-ebb phase (hereafter, ebb refers to the phase when sea level is dropping). Cross-isobath flow also reversed to be upslope, bringing colder (deeper) waters to the lander site.

Lander 6 was located in the NW, close to lander 2 (in the flank) but in a shallower site within a complex topographic site surrounded by rocky outcrops. In this deployment, the dominant circulation was towards N, also aligned with the AC general flow, but a notable westward component was observed. Time series details (Supp. Fig. 3) show that this westward flow is caused by short but intense cross-isobath pulses bringing warm waters to the lander position.

Lander 5 exhibited circulation towards E most of the time, as opposed to the expected AC recirculation, and with a large cross-isobath

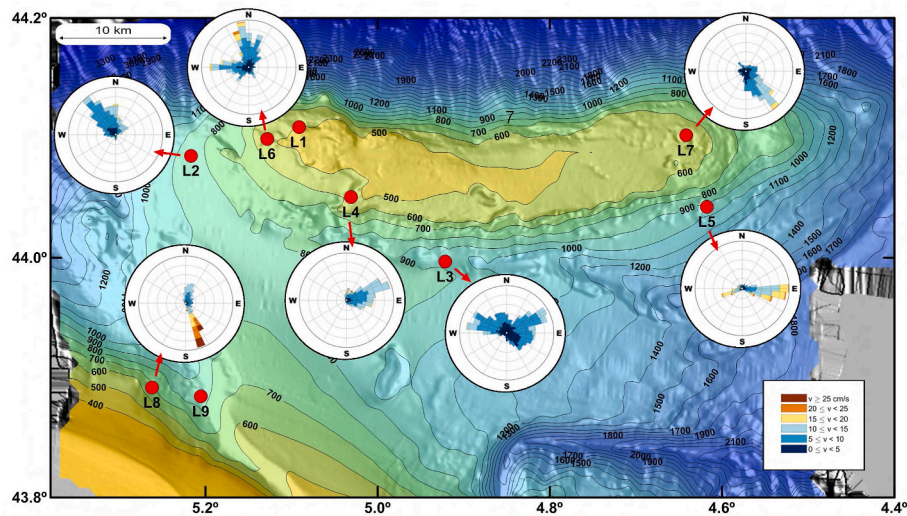


Fig. 5. Map showing location and currents recorded in each lander. Direction, frequency, and strength “Current-rose” composition.

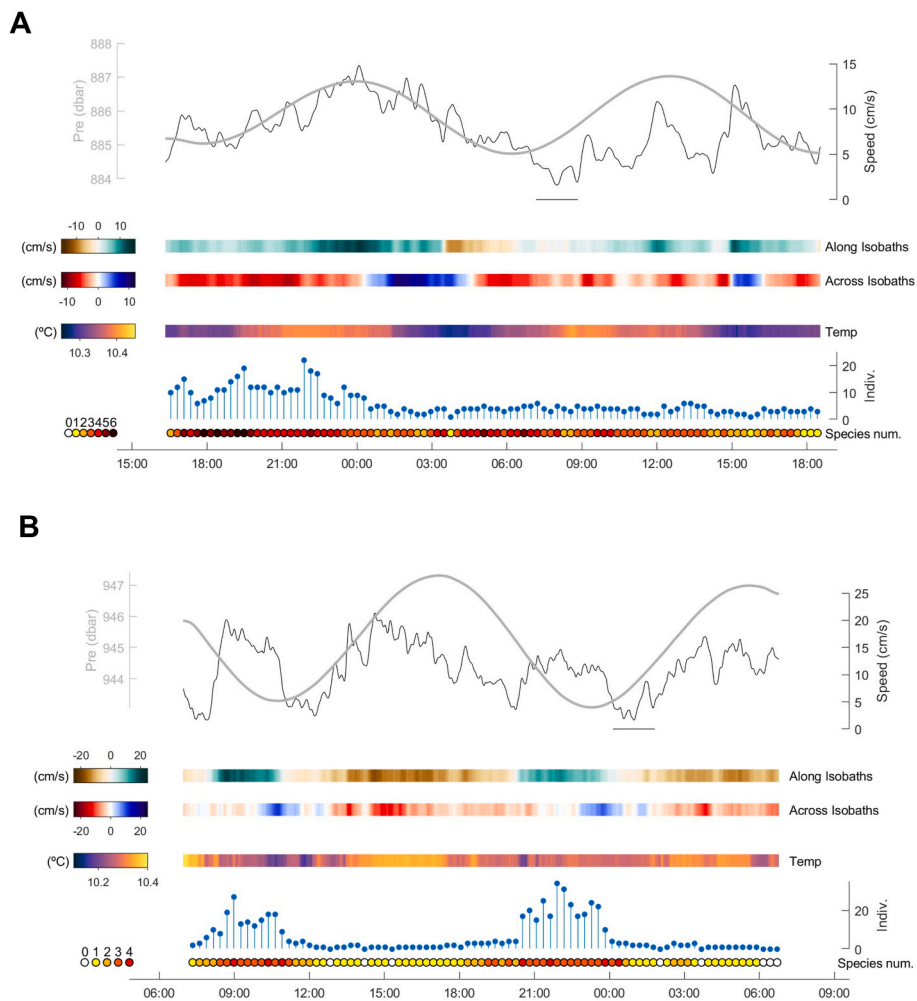


Fig. 6. High-resolution environmental records at (A) lander 2 and (B) lander 5, and species richness and abundance during deployment. In the top figure, current speed (cm s^{-1}) and depth pressure (dbar). In the middle figure, current direction along and across the slope and temperature ($^{\circ}\text{C}$) near the sea floor. In the bottom figure, number of individual and species richness by time interval.

component. Expected along-isobath WSW current was established only for a short time slot of about 3 h within the second half of the ebb phase (Fig. 6B). We cannot establish whether this lander captured a transient

circulation feature or this is indeed a typical tidal cycle pattern. Note that previous studies inferred that the eastern side of the bank was much less capable of establishing persistent recirculation flows than its

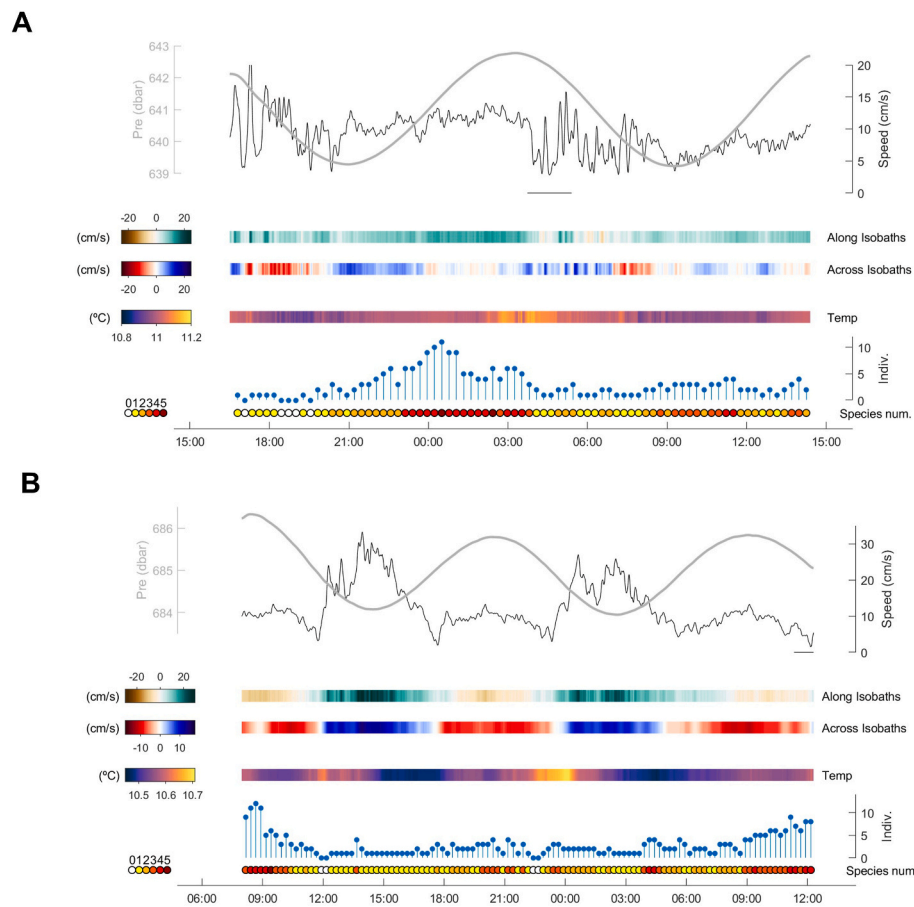


Fig. 7. High-resolution environmental records at (A) lander 4 and (B) lander 8 and species richness and abundance during deployment. In the top figure, current speed (cm s^{-1}) and depth pressure (dbar). In the middle figure, current direction along and across the slope and temperature ($^{\circ}\text{C}$) near the sea floor. In the bottom figure, number of individual and species richness by time interval.

western counterpart, possibly favoring the creation of dipole structures (González-Pola et al., 2012).

Lander 4 was located at a complex topographic incision or canyon that penetrates the southwestern bank summit. Current progressed upcanyon aligned with local topography for the complete tidal cycle, but ebb/flooding phases are distinct. During the ebb phase, strong turbulence developed, exhibiting strong high-frequency shifts in currents (Fig. 7A) and also in the vertical velocities and thermal structure above the lander (not shown). The flooding phase is characterized by a stronger but smooth flow.

Landers 3 and 8 were located at the features known as Le Danois Moat and Gijón Moat, respectively (Liu et al., 2019) (Fig. 1). Lander 3 presented a somewhat symmetric E–W flow aligned with the tidal cycle, with a northwards component; although, the geomorphology studies inferred long-term eastward dominant flow due to the advance of the MOW boundary current (Supp. Fig. 2). Lander 8, on the contrary, presented an intense upcanyon phase during the ebb tidal phase and a gentler and longer downcanyon phase, similar to what was observed in the close Gaviera canyon within the Avilés canyon system (Sánchez et al., 2014). Current speed exhibited current peaks during the ebb tide (Fig. 7B).

Statistics on hydrography and currents for all landers are presented in Table 1. Maximum current speed is indicated whereas minimum current values dropped to zero in all lander. Hydrography was directly related to regional water mass properties at deployment depths. Temperature spans from roughly 11°C at 500 m to 10°C at 1000 m, while salinity rises from c. 35.60 to 35.75 (note that regional salinity maximum is located at the core of Mediterranean waters at around 1000 m). Temperature range due to tidal cycles remained within $0.2\text{--}0.3^{\circ}\text{C}$,

and salinity was less than 0.02. Current strength is more related to surrounding topographic character, typically within the range of $5\text{--}20 \text{ cm s}^{-1}$, with the exception of lander 8, at Gijón moat, peaking over 30 cm s^{-1} .

3.2. Richness, diversity, and abundance

A total of 41 taxa were identified from 10,989 photographs taken during the nine lander deployments (Table 1). The taxa include 12 teleost fishes, 9 elasmobranchs, 11 crustaceans, 6 echinoderms, and 3 mollusks (Supplementary Table 1). Species peak abundance is listed in Table 3. The teleost species observed most frequently was the greater forkbeard (*Phycis blennoides*), which was recorded in all landers, followed by the Kaup's arrowtooth eel (*Synaphobranchus kaupii*), also in terms of number of individuals observed. The species recorded most frequently among the elasmobranchs was the blackmouth catshark (*Galeus melastomus*), and among the invertebrates, the shrimp *Plesionika martia*, scavenger isopods (mainly *Politolana sanchezi*), several species belonging to the genus *Pagurus*, the sea urchin *Araeosoma fenestratum*, and the gastropod *Colus gracilis*.

Fig. 8 shows the cumulative richness of each of the nine landers deployed during the whole period. Differences were found in both number of species and time to reach maximum number. For lander 6, occurrence of species is almost continuous until reaching maximum number in less than 12 h, similarly in lander 9. Conversely, in lander 2, 70% of total richness is achieved within the first 2 h of deployment. In landers 1, 3, 4, 5, and 7, arrival of species was gradual. Highest richness was observed in lander 2 ($n = 18$ species), located in the west flank at a 886-m depth; lowest richness was observed in landers 4 and 7 ($n = 9$ and

Table 3

List of species recorded in each deployment ordered by taxonomic group and following alphabetical order. First arrival time in minutes (t_{arr}) and peak abundance (N_{max}). A list with all taxonomical information is included in the Supplementary Material.

	Species	Lander 1		Lander 2		Lander 3		Lander 4		Lander 5		Lander 6		Lander 7		Lander 8		Lander 9	
		t_{arr}	N_{max}	t_{arr}	N_{max}	t_{arr}	N_{max}	t_{arr}	N_{max}	t_{arr}	N_{max}	t_{arr}	N_{max}	t_{arr}	N_{max}	t_{arr}	N_{max}	t_{arr}	N_{max}
Teleostean	<i>Conger conger</i>	390	1					37	4			691	1	1121	1	17	1		
	<i>Synaphobranchus kaupii</i>			2	20	1	9			3	34							9	3
	<i>Hoplostethus mediterraneus</i>	870	1					159	1										
	<i>Micromesistius poutassou</i>											231	1						
	<i>Nezumia aequalis</i>																	385	1
	<i>Trachyrincus scabrus</i>					903	1									21	1		
	<i>Mora moro</i>			20	2	28	1	9	1	19	3					6	2		
	<i>Phycis blennoides</i>	8	1	58	5	648	2	964	1	70	2	263	1	154	1	56	2	5	5
	<i>Lophius piscatorius</i>					520	1												
	<i>Polyprion americanus</i>											472	1						
	<i>Helicolenus dactylopterus</i>	6	4									136	2						
	Liparidae gen.indet.																		31
Elasmobranchs	<i>Galeus melastomus</i>	56	1	42	1					37	1	87	1			38	1		
	<i>Hexanchus griseus</i>			314	1					880	1	144	1						
	<i>Centrophorus squamosus</i>			486	1	151	1			805	1							10	1
	<i>Dalatias licha</i>																	696	1
	<i>Deania calceus</i>			48	1	67	1												
	<i>Etmopterus spinax</i>	2	1			933	1			178	1	48	1	99	1				
	<i>Centroscymnus coelolepis</i>			122	1	177	2												
	<i>Scymnodon ringens</i>			126	1	949	1			91	1								
	<i>Dipturus nidarosiensis</i> sp. inc.			1472	1	1033	1												
Crustaceans	<i>Cancer bellianus</i>	714	1									1407	1						
	<i>Corystes cassivelaunus</i> sp. inc.															910	1		
	<i>Chaceon affinis</i>								561	2						154	1	321	1
	<i>Paromola cuvieri</i>	70	1	1016	1									784	1				
	<i>Munida sarsi</i>	1	14													1	3		
	<i>Nephrops norvegicus</i>											232	1						
	<i>Bathynectes maravigna</i>	80	4					664	1			475	2	213	2	12	2		
	<i>Pagurus</i> sp. indet.	96	1	90	1			388	1					557	1			46	1
	<i>Plesionika martia</i>			40	1			463	1	4	1	378	2	847	2	216	1	4	1
	<i>Polybius henslowii</i>			654	2														
<i>Politolana sanchezi</i>			32	200	69	700			84	700	181	200	48	100	94	50	117	15	
Echinoderms	<i>Pentametrocrinus atlanticus</i>			0	2														
	<i>Cidaris cidaris</i>	1614	1																
	<i>Gracilechinus acutus</i>			78	1														
	<i>Araeosoma fenestratum</i>	510	2			186	1	216	4							798	2	140	1
	<i>Ophiuroidea</i> ord. indet.			0	2							1202	1	58	14			8	7
<i>Holothuroidea</i> ord. indet.											1203	1					229	1	
Mollusca	<i>Colus gracilis</i>	14	1					379	4			395	3	574	1			152	1
	<i>Antalis</i> sp. indet.															1197	4		
	<i>Gastropoda</i> ord. indet.															918	1	452	2

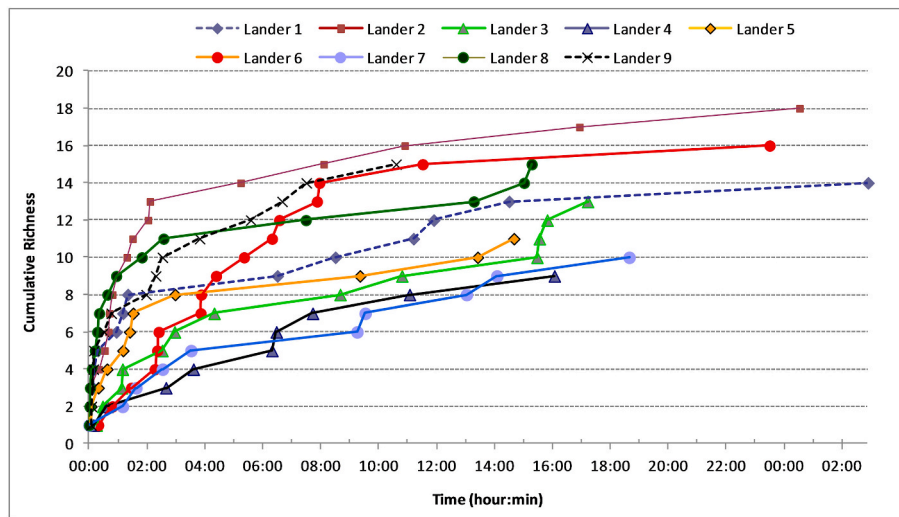


Fig. 8. Cumulative richness by lander according to deployment period.

$n = 10$, respectively), located at the top of the bank at 641- and 551-m depth, respectively.

The main differences found among lander deployments regarding species are related to depth. The landers located at the top of the bank (1, 4, 6, and 7) showed more species in common—*Phycis blennoides*, *Conger conger*, *Helicolenus dactylopterus*, *Etmopterus spinax*—compared with those at deeper stations, although some species appeared only in landers 1 and 4, such as *Hoplostethus mediterraneus* or *Araeosoma fenestratum*. In deeper hauls, the most frequent observed species were *Mora moro* and *Synaphobranchus kaupii*. In particular, the latter was abundant in lander 2 ($N_{max} = 20$) from the beginning to almost the end of the deployment (continuously during the first 9 h) and in lander 5 ($N_{max} = 34$). Except some elasmobranchs such as *Galeus melastomus* and *Etmopterus spinax* which are relative high abundant and show a wide depth distribution, landers located at the top of the bank did not hardly record any elasmobranch species. However, elasmobranchs were identified in deeper stations, mainly landers 2 (highest number of species; $n = 7$), 3, and 5. Species characteristic of deep waters, such as *Centrophorus squamosus*, *Centroscymnus coelolepis*, *Scymnodon ringens*, or *Dipturus nidarosiensis* were among those recorded. Some teleost fishes were observed only in one station; that is the case of *Lophius piscatorius* and *Trachyrinchus scabrous*, identified only in lander 3, *Micromesistius poutassou*, identified only in lander 6, or the elasmobranch *Dalatias licha*, the macrourid *Nezumia* (likely *Nezumia aequalis*), and a specimen belonging to the Liparidae family (likely *Paraliparis membranacea*), all of them species recorded previously in the study area and identified only in lander 9.

Abundance estimates derived from the Priede et al. (1990) and Priede and Merrett (1996) approach are presented in Table 4. Abundance data obtained from previous surveys conducted in the area using otter trawl and beam trawl sampling gears were included for comparative purposes (Sánchez et al., 2008). Currents speed (V_w) used were those corresponding to each lander respectively (Table 1). In landers 1 and 9, V_w data were not recorded; we therefore used V_w values from landers 4 and 8, respectively, due to their location and similarity obtained from cluster analysis. Fish swimming speed (V_f) was not available for most species reported. Therefore, the same approach performed by Priede et al. (1990) was applied: $V_w = V_f$. Only those fish with (V_f) values estimated from previous studies and some invertebrates for whom speed had been calculated in the present study (Section 3.3.) were used instead.

Despite the exhaustive sampling conducted in previous multidisciplinary surveys, prior to the establishment of the MPA, using otter and beam trawl gears, some species such as, *Polyprion americanus* or

Table 4

Abundance estimates (N per km^2) obtained from baited lander (this study) and from trawl gears (Sánchez et al., 2008). M-dash ‘—’ indicates low number and ‘na’ that not data is available for comparison.

Species	Lander	Trawl	Species	Lander	Trawl
<i>Synaphobranchus kaupii</i>	1492.7	735.5	<i>Hexanchus griseus</i>	0.1	na
<i>Mora moro</i>	205.5	366.3	<i>Deania calceus</i>	6.4	108.4
<i>Phycis blennoides</i>	220.0	477.3	<i>Dalatias licha</i>	—	24.5
<i>Micromesistius poutassou</i>	0.2	15101.4	<i>Etmopterus spinax</i>	1421.0	2491.8
<i>Hoplostethus mediterraneus</i>	0.2	310.1	<i>Dipturus nidarosiensis</i>	—	na
<i>Trachyrinchus scabrous</i>	7.2	3785.6	<i>Paromola cuvieri</i>	1.2	na
<i>Lophius piscatorius</i>	—	22.5	<i>Bathymectes maravigna</i>	8.1	549.5
<i>Polyprion americanus</i>	0.04	na	<i>Plesionika martia</i>	446.4	63.5
<i>Helicolenus dactylopterus</i>	157.8	33.5	<i>Chaceon affinis</i>	0.2	3.3
<i>Conger conger</i>	15.2	5.3	<i>Cancer bellianus</i>	—	1.3
<i>Coryphaenoides rupestris</i>	—	97.9	<i>Nephrops norvegicus</i>	0.2	2.6
<i>Galeus melastomus</i>	12.7	3481.5	<i>Munida sp</i>	4905.0	4560.0*
<i>Centrophorus squamosus</i>	8.3	na	<i>Gracilechinus acutus</i>	1.7	248.1
<i>Centroscymnus coelolepis</i>	1.0	1.3	<i>Cidaris cidaris</i>	—	27.8
<i>Scymnodon ringens</i>	1.0	21.8	<i>Colus gracilis</i>	18.9	2241.8

* Two species (*Munida sarsi* + *M. tenuimana*).

Centrophorus squamosus, had not been recorded (Table 4). For other species, the density obtained from the landers in the present study was insignificant compared with previous trawl samplings; this is the case of *Micromesistius poutassou*, *Lophius piscatorius*, or *Hoplostethus mediterraneus*, among others. According to the results obtained in the present study and those obtained from previous surveys, no relation exists between abundance estimates using lander data and those obtained using trawl gears. Only a few species (*Mora moro*, *Etmopterus spinax*, *Chaceon affinis*, *Nephrops norvegicus*) showed relative similar values.

3.3. Species behavior in relation to oceanographic dynamics

Exploring the behavior of species in relation to near-bottom water dynamics represents one of the main targets of the lander design and the

motivation of combined time series figures. However differences were observed among the stations and not a robust or recurrent pattern can be described. Figs. 6 and 7 highlight distinct features. Deployment 2 (Fig. 6A) shows fairly stable environmental conditions and the highest abundance and richness of the species at the beginning of the deployment. Most species arrived in a relatively short time (less than 2 h, Fig. 8), suggesting they came from adjacent areas near the North slope of the bank. Among the species observed in this area is remarkably the presence of elasmobranchs, some arriving fast and others presumably coming from a long distance according to t_{arr} (Table 3). The decaying abundance at the end of the deployment was observed in other landers, such as 3 and 7 (Supplementary figures) or 8 (Fig. 7B); this may be related to bait consumption by small scavengers (mainly *P. sanchezi* and *Natanolana* sp.) and odor loss. Decrease in bait's attractiveness probably affected all deployments.

Interestingly, lander 5 (Fig. 6B) showed two distinct flow patterns and a strong response in appearance of species and their abundance. Current flow was offshore, ESE, most of the time, but shifted to along-slope, towards W, for a short period close to low tide, precisely when species appeared in two defined periods. This indicates that, assuming that the organisms move towards the direction of the bait odor plume, the species swam from the shallower areas of the Le Danois Moat. This channel located in the South flank of the bank used to be a good fishing ground for deep water sharks fishery and five elasmobranchs were recorded at this site (Table 3). It is noteworthy, as it is also observed in lander 2, the presence of the scavenger *P. sanchezi* which is particularly significant during the two periods of positive current towards W, along isobaths. The existence of strong currents in this lander towards very deep areas of the Le Danois Moat and the less number of species recorded suggests a lower biological production in deeper areas of the MPA.

Deployment 4 at the topographic incision (Fig. 7A) is also interesting in terms of faunal behavior. Fishes preferred the more uniform flooding phase instead of the ebb phase, during which, flow was always upslope, presenting enhanced shear and turbulence. One of the main species that frequently appeared in this lander was the European conger eel (*Conger conger*), probably coming from the rocky outcrop located at a short distance towards the W (Fig. 4). This rocky promontory, in which one of the fixed sampling stations for monitoring the conservation status of the MPA is located, is characterized by the presence of a gorgonian forest with a high abundance of this species (Prado et al., 2019).

Deployment 8 at Gijón Moat (canyon-like feature; Fig. 1) showed a major arrival of species within the first 1–2 h and fishes appearing mostly during the smooth down-slope phase at negative along isobaths current (Fig. 7B). Presence of individuals dropped notably when the maximum downcanyon current was well established, almost vanishing by the end of this phase, around 12:00 p.m. and 00:00 a.m. In general terms, and likely due to their mobility, fish species (teleosteans and elasmobranchs) are the first ones to appear and invertebrates showed longer t_{arr} in this area. A similar pattern can be inferred from hydrography in the nearby lander 9 (Supplementary figures), although this deployment lacks currents data.

The scavenger isopod *P. sanchezi* (Frutos and Sorbe, 2010), found in all landers except for landers 1 and 4, was observed in lander 2 during the whole deployment, with high intensity in the second half period—after 13:00 p.m.—coinciding with the flood tide phase. Similar results were observed in landers 7 and 8, in which *P. sanchezi* showed higher abundance after flooding tide peaks.

3.4. Multivariate analysis

An initial matrix of 41 species was reduced to 25 species. Those not identified at species level and those that only appeared in one lander were excluded from the analysis. The hierarchical analysis clearly identified two groups (Fig. 9) at a 45% level of similarity. The first cluster, group A, comprises landers L1, L4, L6, and L7 (498–641-m

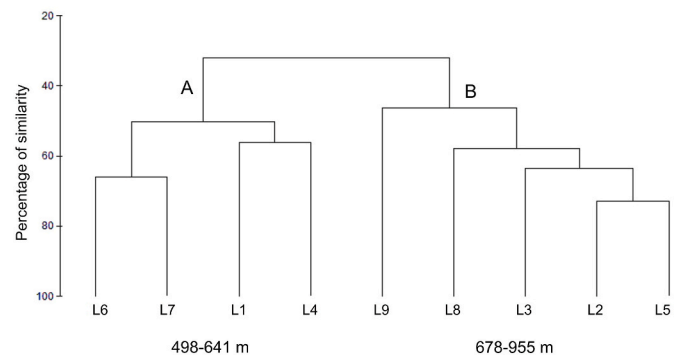


Fig. 9. Faunal zones identified based on group-averaged cluster of Bray–Curtis similarities from species ($n = 25$) using N_{max} data and squared root transformation. Nine landers: Group A (top of the bank) and Group B (slope and intraslope basin).

depth) located at the top of the bank. The second cluster, group B, comprises landers L2, L3, L5 (886 m, 955 m and 945 m depth respectively), located on different positions along the southern flank of the bank showing a 65% level of similarity and and landers L8 and L9, (678–955-m depth), located in the intraslope basin (Fig. 1). Analysis of similarities (ANOSIM) confirmed significance of group separation (global $R = 0.907$, $p = 0.001$).

The similarity percentage (SIMPER) analysis showed the species contributing the most to the divergence between the two groups (Table 5). *S. kaupii* was found only in group B; while *Helicolenus dactylopterus* was found only in group A; *Phycis blennoides* was found in both groups but with higher abundance in group B; whereas *Ophiuroidea* species, *Colus gracilis*, and *Bathynectes maravigna* were more abundant in group A, at the top of the bank. The majority of deep-water elasmobranchs were observed in group B, in the deeper area of the southern flank.

3.5. Biological traits analysis (BTA)

Biological traits analysis (BTA) scores for all species identified in

Table 5

Dissimilarity index between the two groups of landers based on N_{max} and the species that contributed most to this discrepancy.

Species	Average N_{max}		Av. Diss	Diss/SD	Contrib %	Cum. %
	Group 1	Group 2				
<i>Synphobranchus kaupii</i>	0.0	15.0	26.0	1.8	33.2	33.2
<i>Ophiuroidea</i>	3.8	1.4	8.3	0.8	10.6	43.8
<i>Phycis blennoides</i>	1.0	3.2	4.4	1.4	5.7	49.5
<i>Colus gracilis</i>	2.3	0.2	4.1	1.4	5.3	54.7
<i>Bathynectes maravigna</i>	2.3	0.4	3.8	1.5	4.9	59.7
<i>Conger conger</i>	1.8	0.2	3.1	1.0	4.0	63.7
<i>Helicolenus dactylopterus</i>	1.5	0.0	3.1	0.9	4.0	67.6
<i>Araeosoma fenestratum</i>	1.5	0.8	3.1	1.2	3.9	71.5
<i>Politolana sanchezi</i>	1.5	2.0	3.0	1.9	3.9	75.4
<i>Mora mora</i>	0.3	1.6	2.6	1.6	3.3	78.7
<i>Plesionika martia</i>	1.3	0.8	1.7	1.3	2.2	80.9
<i>Centrophorus squamosus</i>	0.0	0.8	1.6	1.8	2.0	82.9
<i>Chaceon affinis</i>	0.0	0.8	1.5	1.2	1.9	84.8
<i>Centrocyttus coelepis</i>	0.0	0.6	1.3	0.7	1.6	86.4
<i>Etmopterus spinax</i>	0.8	0.4	1.1	1.0	1.4	87.8
<i>Pagurus</i> sp.	0.8	0.4	1.1	1.0	1.4	89.2
<i>Scymnodon ringens</i>	0.0	0.6	1.1	1.1	1.4	90.6

landers were obtained according to the criteria presented in Table 2. The percentage of biological trait categories using a baited camera for the study area (all stations) is shown in Fig. 10. The study of animal behavior using landers is more efficient for those swimming or crawling species with high mobility. Fish are usually the first species to appear. The sampling method provides information from a great range of sizes, always greater than 2 cm. Predator and/or scavenger species are more likely to be observed using this method.

3.6. Mobility

Different mobility patterns were observed. Several species, mainly high-mobile species like sharks, (e.g., *Hexanchus griseus*, *Deania calceus*, and *Centrophorus squamosus*) arrived and left. Other species remained in the area during long periods of the time in the proximity of the bait (e.g., *Synapobranchus kaupii*, *Helicolenus dactylopterus*, and *Phycis blenoides*). Although movement of these species could be estimated using images following the method described in section 2.4., their stationary behavior prevents inference of swimming speed (V_f). Thus, velocities of only a few invertebrates were estimated (Table 6). Several species followed a straight line, whereas other showed a more erratic behavior (snails or sea stars). Several species alternated short tracks with stationary periods. Brittle stars (class Ophiuroidea) or squat lobster (*Munida sarsi*) were often observed to bury themselves and keep motionless after covering certain distances.

4. Discussion

Deployment of landers on the deep-sea of El Cachucho MPA has allowed to describe, for the first time, the mobile fauna attracted to bait, 41 species, and its behavior in relation to the oceanographic dynamics in the study area.

4.1. Methodological assumptions

The use and advantages of autonomous landers have been extensively reviewed by Priede and Bagley (2000), Bagley et al. (2004), and Cappelletti et al. (2007), among others. One of the most important benefits of using baited camera or video approaches is that these are nonextractive and do not cause major disturbance to the substrata or its epibenthos. These approaches can therefore be used in marine reserves and rugose

seabed topographies and enable the gathering of information on number and size of animals of special conservation significance (Cappelletti et al., 2007). Large mobile animals who normally avoid extractive fishing gears or scuba divers during visual censuses in shallow waters can also be recorded in such manner (Cappelletti and Brown, 1996 for review).

Deployment duration should always be standardized for comparative purposes. In the present work, one of the objectives was to study the oceanographic dynamics along a daily cycle; thus, duration was set at 24 h as a minimum. Some studies considered 60 min enough time to identify species (Currey-Randall et al., 2020), whereas others have demonstrated 30 min to be sufficient for sampling particular species (Harasti et al., 2015). Nevertheless, most of these studies were conducted in shallow areas or temperate reefs. Cumulative curves can also help to determine the optimal time for camera settings. Even though great variability was observed in cumulative richness among lander deployments in the present work, 80% of total richness was achieved 9 h after mooring and 50% in the first 3.5 h.

Problems of long-time deployments are related to battery duration, store capacity, and bait attraction. Use of still cameras instead of video recording can solve the former two; the latter, however, is more challenging. Due to the important role of bait in attracting organisms, type and quantity should also be standardized to facilitate comparisons. In the present work, locally sourced mackerel (*Scomber scombrus*) and horse mackerel (*Trachurus trachurus*) were used as bait; however, the effect and dispersal of the odor plume during deployment duration remains unknown. This issue must be improved and better controlled in future experiments. Some studies recommend sardine-type oily bait, as the oil disperses to attract fish (Dorman et al., 2012; Langlois et al., 2020).

The main disadvantages of using baited cameras are the limits in the level of taxonomic identification from images (Horton et al., 2016; Sigovini et al., 2016), the fact that some taxa do not come to the bait, that weight of animals cannot be determined directly, and the assumptions made on abundance estimates (Bailey et al., 2007; Stoner et al., 2008). In particular the main difficulties of this approach for population density estimation are the selective observation of only scavengers and the large number of assumptions required for the estimation regarding diffusion of the odor plume, foraging strategy of individuals, or swimming speed (Bailey et al., 2007). However, repeated standardized experiments can partially solve these problems and be an additional tool for monitoring a MPA.

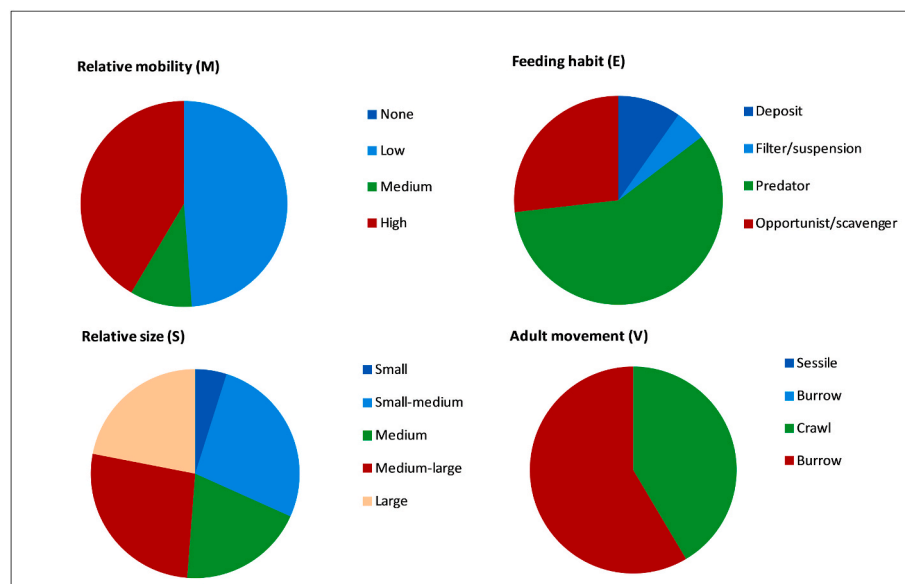


Fig. 10. Percentage of biological trait categories used to describe ecological functioning in the species sampled using baited camera.

Table 6

Distance covered (m) and movement rates ($\text{cm}\cdot\text{s}^{-1}$) of some invertebrate species observed during lander deployments. Mean and maximum distance and speed recorded for each frame series and the average and the standard deviation (SD) for the whole number of observations.

	SPECIES	Lander	Frames Serie	N° observ	Time (min)	Track covered (m)	Distance (m) and speed (cm/s) by frame				Speed (cm. s^{-1}) Average (\pm SD)	Direction				Observations
							Mean distance	Max	Mean	Max		Circle	Line	Erratic	Buried	
CRUSTACEANS	<i>Bathynectes maravigna</i>	1	651–655	4	10	2.03	0.51	0.66	0.42	0.55						Occasionally observed swimming not crawling
		8	70–78	8	9	4.12	0.51	0.87	0.86	1.44	0.66 \pm 0.22			X		
	<i>Cancer bellianus</i>	1	81–84	3	4	1.26	0.42	0.61	0.70	1.02						Occasionally stops or buried
		4	686–705	6	12	5.02	0.84	1.68	0.7	1.40	0.70			X		
		657–663	6	9	0.777	0.13	0.331	0.14	0.37							
		670–678	9	14	0.557	0.06	0.177	0.07	0.20							
	<i>Pagurus sp.</i>	9	423–430	6	6	0.33	0.05	0.07	0.09	0.12	0.09 \pm 0.03			X	X	
			456–459	3	3	0.14	0.05	0.05	0.08	0.08						
MOLLUSKS	<i>Munida sarsi.</i>	8	520–536	15	15	0.58	0.04	0.06	0.07	0.10						Intermittent movement with stops Regularly following a straight line. sometimes oblique Oblique line Circular Oblique line
			42–47	5	5	0.44	0.11	0.18	0.18	0.30	0.21 \pm 0.04			X		
		66–70	4	4	0.59	0.15	0.25	0.24	0.42	0.04						
		837–841	4	6	0.72	0.18	0.20	0.20	0.22	0.15 \pm 0.04			X			
	<i>Colus gracilis</i>	6	282–287	6	9	0.52	0.09	0.12	0.10	0.13						Regularly following a straight line. sometimes oblique Oblique line Circular Oblique line
		7	590–600	10	10	0.70	0.08	0.11	0.13	0.18				X		
		7	602–614	12	12	0.72	0.07	0.11	0.11	0.18			X			
ECHINODERMS	<i>Gracilechinus acutus</i>	2	807–811	5	5	0.32	0.10	0.11	0.17	0.18				X		
			80–97	17	34	1.10	0.07	0.10	0.06	0.09	0.06 \pm 0.02			X		
	<i>Cidaris cidaris</i>	1	837–843	6	12	0.27	0.04	0.07	0.04	0.06	0.04 \pm 0.01			X		Occasionally semicircular line Frequently following a straight line. Sometimes oblique
			936–960	27	54	1.19	0.04	0.09	0.04	0.08	0.01					
	<i>Araeosoma frenestratum</i>	4	147–164	18	26	2.85	0.13	0.21	0.19	0.23						Frequently following a straight line. Sometimes oblique
			172–182	10	14	1.72	0.29	0.46	0.21	0.51	0.23 \pm 0.09			X		
	<i>Ophiuroidea</i>	7	657–673	8	9	0.87	0.14	0.75	0.16	0.40						Occasionally with stops and buried
			850–854	6	6	1.35	0.33	0.39	0.37	0.43						
		1170–1176	5	5	0.20	0.04	0.08	0.07	0.13							
		1410–1412	3	3	0.53	0.18	0.21	0.29	0.36	0.16 \pm 0.12			X	X		
			1428–1439	12	12	0.77	0.06	0.21	0.11	0.36						

4.2. Species assemblages and abundance

Baited cameras have been demonstrated to perform well in both reefs and shallow areas (Eliis and DeMartini, 1995; Willis et al., 2000; Stoner et al., 2008) and in deep sea (Priede et al., 1990; Priede and Merrett, 1996; Yau et al., 2001; King et al., 2006).

Most species observed in the present study have been reported in previous studies using baited cameras in the Bay of Biscay (Guennegan and Rannou, 1979; Mahau et al., 1990), in adjacent deepwater areas (Priede I et al., 1994; Bagley et al., 1994; Jones et al., 1998; Linley et al., 2016), or in the Mediterranean Sea (Jones et al., 2003; D'Onghia et al., 2004; Linley et al., 2018). Among the species frequently reported in these studies are chondrichthyans such as; *Hexanchus griseus*, *Etmopterus spinax*, and *Galeus melastomus* and teleost fishes such as; *Synphobranchius kaupii*, *Phycis blennoides*, *Mora moro* and *Coryphaenoides rupestris* (Uiblein et al., 2003; Trenkel et al., 2004; Lorance et al., 2000). These species show wide spatial distributions and their presence is relatively frequent in deep waters.

In the present study, abundance estimates obtained from a baited camera based on time of first arrival (t_{arr}) did not provide good indication of prevailing abundance. As has been noted by Yau et al. (2001), the inverse relationship between abundance and the square of the average arrival time (t_{arr}) in Priede's model is problematic because small changes in arrival time cause major changes in theoretical density estimates. In the present study, no relationship has been found between t_{arr} and depth; however, the studied depth range was only 500–950 m. Previous research in the Mediterranean Sea and in the Atlantic Ocean have found a positive relationship between t_{arr} and depth with a large studied depth range of 500–5000 m (Linley et al., 2018).

Which metrics are more appropriate for abundance estimates when using baited cameras has been debated for a long time (Priede and Merrett, 1996; Cappo et al., 2004). Maximum number of fish N_{max} is a widely used estimator of relative abundance (Willis et al., 2000; Whitmarsh et al., 2017) as this is conservative and ensures no individual is counted more than once (Schobernd et al., 2014). Its use has been reviewed in detail by Cappo et al. (2003, 2004). Other metrics have been proposed using video techniques in areas of high population densities of a certain species (Stobart et al., 2015).

BRUVs have been shown to be more efficient than traps for sampling tropical continental shelf demersal fishes (Harvey et al., 2012). However, a comparison of baited underwater cameras and longlines for assessing the composition of deepwater fish assemblages off south-eastern Australia showed BRUVs to be a less effective means of sampling (McLean et al., 2014).

Abyssal and shallow studies have shown a marked divergence in indices of abundance (Cappo et al., 2007). Mean arrival times in shallow deployments occur at the level of seconds to minutes rather than tens of minutes to hours in abyssal studies. In the present study, first arrival times range from 1 to 2 min to near 1 h, with *S. kaupii* as one of the first species to arrive in several deployments.

Recent research has presented models that could improve the relation between fish counts and population size (Farnsworth et al., 2007; Campbell et al., 2015). Mean count has also been tested and compared with N_{max} ; both indexes prevent over counting, however the former inflates the number of zero observations (Campbell et al., 2015). According to these authors, mean count is linearly related to true abundance, while N_{max} shows a power relationship. In spite of this, N_{max} would still be preferable since the average observed abundance for most species are well below the point where nonlinearity becomes a concern.

The differences observed in the present work in time of first arrival among different stations clearly indicates that other factors can have a strong effect. Some of these environmental factors such as, depth, tide phase, and velocity or current direction, are commented below. Others might be related to bait attraction and behavior of species; these key factors in this type of studies can lead to biases in predatory or scavenging species surveyed (Harvey et al., 2007; Yeh and Drazen, 2011;

Jones et al., 2021).

As Bremner et al. (2006) indicate, BTA can be applied to monitor large geographical scales. This method is relatively easy to apply and can be incorporated in the monitoring management of MPAs and in the new proposed areas (Site of Community Importance, SCI) of Nature (2000) network.

4.3. Hydrographic dynamics

The snapshots of current fields gathered by the landers in the present work helped to understand species behavior in relation to environmental conditions, but these are too short to provide a robust standalone description of these dynamics. However, their interpretation together with our previous understanding of Le Danois bank functioning (González-Pola et al., 2012) provided a consistent view. Overall, the AC background circulation along the bank flanks is robust and mostly overcomes the tidal rhythms. The lander at the southeastern side of the bank dynamics provided an intriguing outcome, being the current for most records sweeping outwards from the bank summit. Description of circulation patterns at this part of the bank had been evasive in previous studies. Landers 3 and 8, located at Moats, and lander 4, located in an irregular incision into the bank summit, provided a much stronger response linked to tidal dynamics, which is an expected behavior of canyons in the region (Sánchez et al., 2014) due to flow compression.

4.4. Movements

Information on the movement and connectivity patterns is scarce for many species, especially for invertebrates. Besides most studies investigating this are conducted in shallow areas (intertidal, mangrove habitats, etc.), not in deeper waters. Regarding sea urchins, estimates of movements are available for some species but not for the studied ones in the present work: estimates of daily displacement of *Strongylocentrotus droebachiensis* are 0.5–0.6 m per day (Lauzon-Guay et al., 2006); speed values reported for *Paracentrotus lividus* range between 0.02 cm min⁻¹ (0.003) during daytime and 0.13 cm min⁻¹ during night time (Hereu, 2005) with peaks of 0.66 cm min⁻¹ (Dance, 1987), showing movement to be greater at night. Estimated values obtained in the present work for *Cidaris cidaris* (0.048 cm s⁻¹) and *Araeosoma fenestratum* (0.19 cm s⁻¹) show higher movement rates compared with those for shallower species, and a linear pattern is observed in successive moves.

A tagging experiment conducted on *Buccinum undatum* showed average movement rate to be 0.20 cm s⁻¹ (Himmelman, 1988). This value is similar to those obtained for *Colus gracilis* in the present study, although the size of this species is smaller compared with that of *B. undatum*. Movement patterns of both molluscs are also similar. *Colus* individuals become active when they perceive the odor of food, even if they were buried. The environmental variables associated with movement of this species in the present study are related to high tide and low current speed.

Little is known of movement patterns or distances travelled by hermit crabs, although a few estimates have been obtained for subtidal species and land hermit crabs (Stachowitsch, 1979; Hazlett, 1983; Barnes, 2003). The reported average speed of a hermit crab (genus *Paguristes*) in previous cited studies is 2.1 m h⁻¹, and the reported average distance covered is 21.6 m per day (Stachowitsch, 1979). Hermit crabs make interrupted movements, probably to examine structures in the sediment; thus this issue must be considered when estimating real speed or distance covered. According to previously cited studies, crabs often dig in both mud and sand and remain buried for a certain amount of time before restarting their locomotion. This movement pattern has also been observed in the present study, not only in hermit crabs but also in brittle stars (class Ophiuroidea). Movement rate estimated for hermit crabs of the genus *Pagurus* recorded in the present work was 0.09 (±0.03) cm s⁻¹ (Table 6). In the east coast of the United States, the reported estimated locomotion rate for shallow hermit crab (*Pagurus*

longicarpus) was 2.2 m min^{-1} (3.6 cm s^{-1}) (Tricarico and Gherardi, 2006), comparable to the reported speed of radio-tracked *Clibanarius longitarsus* in an East African mangrove swamp (2.5 m min^{-1} ; 4.16 cm s^{-1}) (Gherardi et al., 1990) but decidedly faster than that of *Clibanarius erythropus* in the Mediterranean shore ($0.5\text{--}5 \text{ cm min}^{-1}$; $0.0083\text{--}0.083 \text{ cm s}^{-1}$) (Benvenuto et al., 2003).

According to the study by Ramsay et al. (1997), none of the scavenger species observed (hermit crabs, swimming crabs, whelks) showed any patterns in abundance related to changes in the tide phase. Results obtained from lander deployments in the present study cannot determine a definitive pattern due to the differences between stations. However, *Colus gracilis* and *Pagurus* species were moderately related to the tide and current speed. The only observation of *Gracilechinus acutus* indicates a preference for low tide and high current speed (similar to *Ophiuroidea* species), whereas this relation was variable in the observations of sea urchin *Araeosoma fenestratum*.

Increased current speed decreased the bait area of attraction for whelks in previous research (Himmelman, 1988; McQuinn et al., 1988), contradicting our observations. A study in which the shape of an odor plume was modelled suggests that fewer scavengers per unit of time might be attracted at lower current speed values (Sainte-Marie and Hargrave, 1987).

The bioturbating and scavenging behavior of *P. sanchezi* has been described by Frutos and Sorbe (2010). This species spends most of its time superficially buried in the substratum, from which emerges opportunistically in response to food odor detected in the overlying water. During lander deployments, a peak in abundance of this species was observed following the arrival of some predator, such as sharks. A high number of individuals were probably hidden inside the flesh of the bait, and in response to a predator attack, they moved away and came back when the predator left. Presence of species inside the flesh of the recovered bait supports this feeding behavior.

Movement rates of several teleost fish observed in our images were not estimated since movement is strongly affected by the foraging behavior of the species. Species observed, such as *Synaphobranchus kaupii*, *Helicolenus dactylopterus*, *Phycis blennoides*, or *Mora moro* respond to the sit-and-wait foraging strategy described by Bailey and Priede (2002). Movement rates cannot therefore be interpreted as swimming rates (Fig. 11). Linley et al. (2016) reported that *Conger conger* was able

to remove large sections of bait and move out of view to consume them. This behavior prevents accumulation of this species in front of the cameras and lead to a N_{max} value rarely above one (Linley et al., 2016).

The teleost *Helicolenus dactylopterus* is a typical sit-and-wait predator feeding mainly on benthic crustaceans, fish, and plankton organisms (Consoli et al., 2010). In most of our images, this species appears resting on the seabed. As it has been reported this fish uses a wide range of habitats and is closely associated with the bottom (Uiblein et al., 2003; Costello et al., 2005; D'Onghia et al., 2014, 2016).

The fact that some species are attracted by baited cameras yielded information on large mobile species such as elasmobranchs that are not frequently capture with extractive fishing gears like trawls. Several studies provide swimming speed of fish (Hoar and Randall, 1978); however, most of these studies are based on laboratory experiments conducted with certain species. To estimate abundance, swimming speed (V_f) values of fish species, such as *Centrophorus squamosus* (8.8 cm s^{-1}), *Hexanchus griseus* (4.8 cm s^{-1}), and *Synaphobranchus kaupii* (5.4 cm s^{-1}) were obtained from published studies conducted in the area (Rodríguez-Cabello and Sánchez, 2014; Rodríguez-Cabello et al., 2018; Uiblein et al., 2002). Estimates of shark swimming speed were based on electronic tagging data. According to Uiblein et al. (2002), a substantial proportion of *S. kaupii* was observed to remain stationary, but swimming estimates (5.4 cm s^{-1}) were based on active and drifting individuals observed in bait experiments.

In conclusion, we consider that the use and development of these noninvasive methodologies based on multiparametric platforms represent an important source of complementary information to monitor the conservation status of vulnerable ecosystems. Their deployment over long periods of time can provide the necessary information to explain the consequences of certain effects of environmental variability that can compromise the survival and species presence in the area.

CRediT authorship contribution statement

Francisco Sánchez: Funding acquisition, Investigation, Methodology, Supervision, Writing – original draft, Data curation, Formal analysis, Writing – review & editing. **Cesar González-Pola:** Data curation, Investigation, Methodology, Software, Formal analysis, Writing – review & editing. **Augusto Rodríguez-Basalo:** Formal analysis, Methodology,

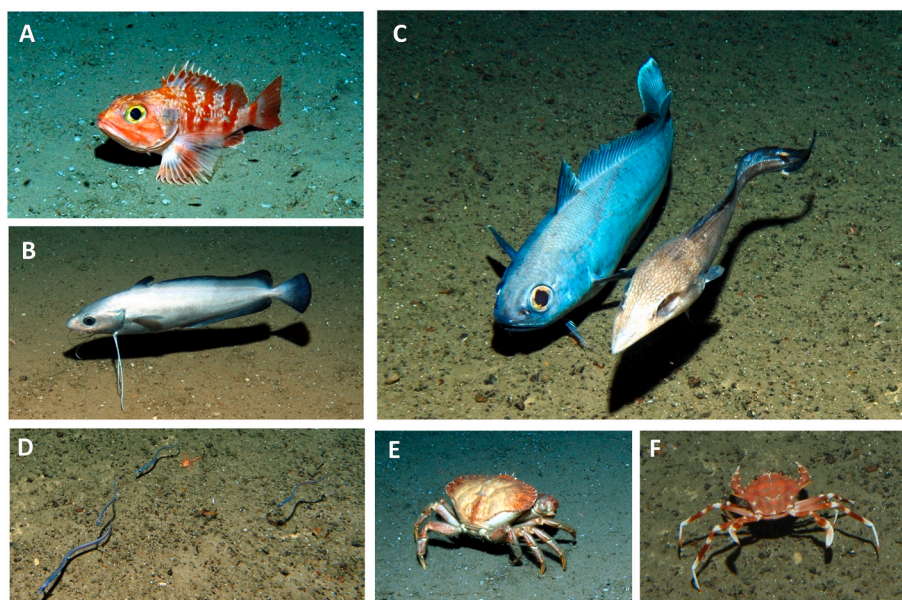


Fig. 11. Images of some representative species observed in landers. (A) Blackbelly rosefish (*Helicolenus dactylopterus*). (B) A greater forkbeard (*Phycis blennoides*). (C) Two teleost fishes: the gadiforme (*Mora moro*) and the macrourid (*Trachyrincus scabrurus*). (D) Three individuals of Kaup's arrowtooth eel (*Synaphobranchus kaupii*). (E) The common deep sea crab (*Cancer bellianus*). (F) Other typical crab (*Bathynectes maravigna*).

Investigation. **Juan Manuel Rodríguez:** Methodology. **Elena Prado:** Formal analysis, Methodology, Software. **Larissa Módica:** Formal analysis, Methodology, Investigation. **Cristina Rodríguez-Cabello:** Formal analysis, Investigation, Methodology, Writing – original draft, Writing – review & editing.

Declaration of competing interest

The authors declare that they have no known competing financial interests or personal relationships that could have appeared to influence the work reported in this paper.

Data availability

The data that has been used is confidential.

Acknowledgements

We are very grateful to some colleagues for their taxonomic expertise, which helped us to identify some of the species in this study; in particular Dr. Sergio Gofas (molluscs) and Dr. Joan Cartes (crustaceans). We also thank the crew of the RV Angeles Alvaríño and the RV Ramón Margalef for their help. This study was cofunded by the Spanish Ministry of Environment through a management agreement with the Spanish Institute of Oceanography (IEO) and was included in the ESMARES2 project.

Appendix A. Supplementary data

Supplementary data to this article can be found online at <https://doi.org/10.1016/j.ecss.2022.108078>.

References

- Altuna, A., 2013. Scleractinia (Cnidaria: Anthozoa) from ECOMARG 2003, 2008 and 2009 expeditions to bathyal waters off north and northwest Spain (northeast Atlantic). *Zootaxa* 3641 (2), 101–128.
- Bagley, P.M., Priede, I.G., Jamieson, A.J., Bailey, D.M., Battle, E.J.V., Henriques, C., Kemp, K.M., 2004. Lander techniques for deep ocean biological research. *Underw. Technol.* 26, 3–12.
- Bailey, D.M., Priede, I.G., 2002. Predicting fish behaviour in response to abyssal food-falls. *Mar. Biol.* 141, 831–840. <https://doi.org/10.1007/s00227-002-0891-9>.
- Bailey, D.M., King, N.J., Priede, I.G., 2007. Cameras and carcasses: historical and current methods for using artificial food falls to study deep-water animals. *Mar. Ecol. Prog. Ser.* 350, 179–191. ISSN 1616–1599.
- Barnes, D.K.A., 2003. Ecology of subtropical hermit crabs in SW Madagascar: short range migrations. *Mar. Biol.* 142, 549–557.
- Benvenuto, C., Sartoni, G., Gherardi, F., 2003. Foraging behaviour of the hermit crab *Clibanarius erythropus* in a Mediterranean shore. *J. Mar. Biol. Assoc. U. K.* 83, 457–461.
- Bremner, J., Rogers, S.I., Frid, C.L.J., 2006. Methods for describing ecological functioning of marine benthic assemblages using biological traits analysis (BTA). *Ecol. Indicat.* 6, 609–622.
- Campbell, M.D., Pollack, A.G., Gledhill, C.T., Switzer, T.S., DeVriese, D.A., 2015. Comparison of relative abundance indices calculated from two methods of generating video count data. *Fish. Res.* 170, 125–133. <https://doi.org/10.1016/j.fishres.2015.05.011>.
- Cappo, M., Brown, I., 1996. Evaluation of Sampling Methods for Reef Fish Populations of Commercial and Recreational Interest. CRC Reef Research Centre, Technical Report No. 6. CRC Reef Research Centre, Townsville, p. 72.
- Cappo, M., Harvey, E., Malcolm, H., Speare, P., 2003. Potential of video techniques to monitor diversity, abundance and size of fish in studies of Marine Protected Areas. In: Beumer, J.P., Grant, A., Smith, D.C. (Eds.), 'Aquatic Protected Areas - what Works Best and How Do We Know?' World Congress on Aquatic Protected Areas Proceedings, pp. 455–464. Cairns, Australia, August 2002.
- Cappo, M., Speare, P., Death, G., 2004. Comparison of baited remote underwater video stations (BRUVS) and prawn (shrimp) trawls for assessments of fish biodiversity in inter-reefal areas of the Great Barrier Reef Marine Park. *J. Exp. Mar. Biol. Ecol.* 302, 123–152. <https://doi.org/10.1016/j.jembe.2003.10.006>.
- Cappo, M., Harvey, E., Shortis, M., 2007. Counting and measuring fish with baited video techniques - an overview. In: Lyle, J.M., Furlani, D.M., Buxton, C.D. (Eds.), Cutting-edge Technologies in Fish and Fisheries Science. Australian Society for Fish Biology Workshop Proceedings; 2006, vols. 28–29. Hobart, Tasmania, pp. 110–114. August.
- Consoli, P., Battaglia, P., Castriota, L., Esposito, V., Romeo, T., Andaloro, F., 2010. Age, growth and feeding habits of the bluemouth rockfish, *Helicolenus dactylopterus dactylopterus* (Delaroche 1809) in the central Mediterranean (southern Tyrrhenian Sea). *J. Appl. Ichthyol.* 26 (4), 583–591. <https://doi.org/10.1111/j.1439-0426.2010.01467.x>.
- Costello, M.J., McCrear, M., Freiwald, A., Lundälv, T., Jonsson, L., Bett, B.J., van Weering, T.C.E., de Haas, H., Roberts, J.M., Allen, D., 2005. Role of cold-water *Lophelia pertusa* coral reefs as fish habitat in the NE Atlantic. In: Freiwald, A., Roberts, J.M. (Eds.), Cold-Water Corals and Ecosystems. Springer-Verlag, Berlin, pp. 771–805. https://doi.org/10.1007/3-540-27673-4_41.
- Clarke, K.R., Warwick, R.M., 2001. Change in Marine Communities: an Approach to Statistical Analysis and Interpretation, second ed. Natural Environment Research Council, Plymouth Marine Laboratory, Plymouth, p. 144.
- Currey-Randall, L.M., Cappo, M., Sempfordorfer, C.A., Farabaugh, N.F., Heupel, M.R., 2020. Optimal soak times for baited remote underwater video station surveys of reef-associated elasmobranchs. *PLoS One* 15, e0231688. <https://doi.org/10.1371/journal.pone.0231688>.
- Dance, C., 1987. Patterns of activity of the sea urchin *Paracentrotus lividus* in the Bay of Port-cros (var, France, mediterranean). *P.S.Z.N.I. Mar. Ecol.* 8, 131–142.
- D'Onghia, G., Politou, C., Bozzano, A., Lloris, D., Rotllant, G., Sion, L., Mastrototaro, F., 2004. Deep-water fish assemblages in the Mediterranean Sea. *Sci. Mar.* 68, 87–99. <https://doi.org/10.3989/scimar.2004.68s387>.
- D'Onghia, G., Capezzuto, F., Carluccio, A., Carlucci, R., Giove, A., Mastrototaro, F., Panza, M., Sion, L., Tursi, A., Maiorano, P., 2014. Exploring composition and behaviour of fish fauna by in situ observations in the bari canyon (southern Adriatic sea, central mediterranean). *Mar. Ecol.* 1–16. ISSN 0173-9565.
- D'Onghia, G., Duineveld, G., Shields, M.A., Sion, L., Tursi, A., Priede, I.G., 2016. Effects of Cold-Water Corals on Fish Diversity and Density (European Continental margin: Arctic, NE Atlantic and Mediterranean Sea): Data from Three Baited Lander Systems. Deep-Sea Research Part II. <https://doi.org/10.1016/j.dsr2.2015.12.003i>.
- Dorman, S.R., Harvey, E.S., Newman, S.J., 2012. Bait effects in sampling coral reef fish assemblages with stereo-BRUVs. *PLoS One* 7 (7), e41538. <https://doi.org/10.1371/journal.pone.0041538>.
- Eliis, D.M., DeMartini, E.E., 1995. Evaluation of a video camera technique for indexing abundances of juvenile pink snapper, *Pristipomoides filamentosus*, and other Hawaiian insular shelf fishes. *Fish. Bull.* 93, 67–77.
- Farnsworth, K.D., Thygesen, U.H., Ditlevsen, S., King, N.J., 2007. How to estimate scavenger fish abundance using baited camera data. *Mar. Ecol. Prog. Ser.* 350, 223–234.
- Froese, R., Pauly, D. (Eds.), 2019. FishBase. World Wide Web electronic publication. www.fishbase.org. version (12/2019).
- Frutos, I., Sorbe, J.C., 2010. *Politolana sanchezi* sp. nov. (Crustacea: Isopoda: Cirrolanidae), a new benthic bioturbating scavenger from bathyal soft-bottoms of the southern Bay of Biscay (northeastern Atlantic Ocean). *Zootaxa* 2640, 20–34.
- Gherardi, F., Micheli, F., Vannini, M., 1990. Movement patterns and dispersal of the hermit crab *Clibanarius longitarsus* in a mangrove swamp. *Mar. Behav. Physiol.* 16, 209–223.
- González-Pola, C., Díaz del Río, G., Ruiz-Villarreal, M., Sánchez, R.F., Mohn, Ch., 2012. Circulation patterns at Le Danois bank, an elongated shelf-adjacent seamount in the Bay of Biscay. *Deep-Sea Res. Part 1* 60, 7–21.
- Guennegan, Y., Rannou, M., 1979. Semi-diurnal rhythmic activity in deep-sea benthic fishes in the Bay of Biscay. *Sarsia* 64 (1–2), 113–116. <https://doi.org/10.1080/00364827.1979.10411372>.
- Harasti, D., Malcolm, H., Gallen, C., Coleman, M.A., Jordan, A., Knott, N.A., 2015. Appropriate set times to represent patterns of rocky reef fishes using baited video. *J. Exp. Mar. Biol. Ecol.* 463, 173–180. <https://doi.org/10.1016/j.jembe.2014.12.003>.
- Harvey, E.S., Cappo, M., Butler, J.J., Hall, N., Kendrick, G.A., 2007. Bait attraction affects the performance of remote underwater video stations in assessment of demersal fish community structure Marine. *Ecol. Progress Series.* 350, 245–254. <https://doi.org/10.3354/meps07192>.
- Harvey, E.S., Newman, S.J., McLean, D.L., Cappod, M., Meeuwig, J.J., Skepper, C.L., 2012. Comparison of the relative efficiencies of stereo-BRUVs and traps for sampling tropical continental shelf demersal fishes. *Fish. Res.* 125 (126), 108–120.
- Hazlett, B.A., 1983. Daily movement in the hermit crabs *Clibanarius tricolor* and *Calcinus tibicen*. *J. Crustac Biol.* 3, 223–234.
- Heredia, B., Pantoja, J., Tejedor, A., Sánchez, F., 2008. El Cachucho, un oasis de vida en el Cantábrico. La primera gran área marina protegida en España. *Ambienta* 76, 10–17.
- Hereu, B., 2005. Movement patterns of the sea urchin *Paracentrotus lividus* in a marine reserve and an unprotected area in the NW Mediterranean. *Mar. Ecol.* 26, 54–62.
- Hernández-Molina, F.J., Wählin, A., Bruno, M., Ercilla, G., Llave, E., Serra, N., Rosón, G., Puig, P., Rebesco, M., Van Rooij, D., Roque, D., González-Pola, C., Sánchez, F., Gómez, M., Preu, B., Schwenk, T., Hanebuth, T.J.J., Sánchez, R.F., García-Lafuente, J., Brackenridge, R.E., Juan, C., Stow, D.A.V., Sánchez-González, J.M., 2016. Oceanographic processes and morphosedimentary products along the Iberian margins: a new multidisciplinary approach. *Mar. Geol.* 378, 127–156. <https://doi.org/10.1016/j.margeo.2015.12.008>.
- Himmelman, J.H., 1988. Movement of whelks (*Buccinum undatum*) towards a baited trap. *Mar. Biol.* 97, 521–531.
- Hoar, W., Randall, D. (Eds.), 1978. Fish Physiology. Locomotion, vol. 7. Academic Press, ISBN 9780080585277, pp. 1–576.
- Horton, T., Marsh, L., Bett, B.J., Gates, A.R., Jones, D.O.B., Benoist, N.M.A., Pfeifer, S., Simon-Lledó, E., Durden, J.M., Vandepitte, L., Appeltans, W., 2021. Recommendations for the standardisation of open taxonomic nomenclature for image-based identifications. *Front. Mar. Sci.* 8, 620702 <https://doi.org/10.3389/fmars.2021.620702>.

- Iorga, M.C., Lozier, M.S., 1999. Signatures of the Mediterranean outflow from a North Atlantic climatology 1. Salinity and density fields. *J. Geophys. Res.* 104 (C11), 25985–26009.
- Jones, E.G., Collins, M.A., Bagley, P.M., Addison, S., Priede, I.G., 1998. The fate of cetacean carcasses in the deep-sea: observations on consumption rates and succession of scavenging species in the abyssal north-east Atlantic. *Proc. Roy. Soc. Lond. B* 265, 1119–1127.
- Jones, E.G., Tselepidis, A., Bagley, P.M., Collins, M.A., Priede, I.G., 2003. Bathymetric distribution of some benthic and benthopelagic species attracted to baited cameras and traps in the deep eastern Mediterranean. *Mar. Ecol. Prog. Ser.* 251, 75–86.
- Jones, R.E., Griffin, R.A., Herbert, R.J.H., Unsworth, R.K.F., 2021. Consistency is critical for the effective use of baited remote video. *Oceans* 2, 215–232. <https://doi.org/10.3390/oceans2010013>.
- King, N., Bagley, P.M., Priede, I.G., 2006. Depth zonation and latitudinal distribution of deep-sea scavenging demersal fishes of the Mid-Atlantic Ridge, 42 to 53°N. *Mar. Ecol. Prog. Ser.* 319, 263–274.
- Langlois, T., Goetze, J., Bond, T., et al., 2020. A field and video annotation guide for baited remote underwater stereo-video surveys of demersal fish assemblages. *Methods Ecol. Evol.* 1–9. <https://doi.org/10.1111/2016-210X.13470>, 2020;00.
- Lauzon-Guay, J.S., Robert, P., Scheibling, E., Barbeau, M.A., 2006. Movement patterns in the green sea urchin, *Strongylocentrotus droebachiensis*. *J. Mar. Biol. Assoc. U. K.* 86, 167–174.
- Le Danois, E., 1948. In: Payot (Ed.), *Les Profondeurs de la Mer*, p. 303. Paris.
- Linley, T.D., Lavaley, M., Maiorano, P., Bergman, M., Capezuto, F., Cousins, N.J., D'Onghia, G., Duineveld, G., Shields, M.A., Sion, L., Tursi, A., Priede, I.G., 2016. Effects of cold-water corals on fish diversity and density (European continental margin: Arctic, NE Atlantic and Mediterranean Sea): Data from three baited lander systems. *Deep-Sea Res. Part II*. <https://doi.org/10.1016/j.dsr2.2015.12.003i>.
- Linley, T.D., Craig, J., Jamieson, A.J., Priede, I.G., 2018. Bathyal and abyssal demersal bait-attending fauna of the Eastern Mediterranean Sea. *Mar. Biol.* 165 (10), 159.
- Liu, S., Van Rooij, D., Vanderpe, T., González-Pola, C., Ercilla, G., Hernández-Molina, F. J., 2019. Morphological features and associated bottom-current dynamics in the Le Danois Bank region (southern Bay of Biscay, NE Atlantic): a model in a topographically constrained small basin. *Deep Sea Res. Oceanogr. Res. Pap.* 149, 103054 <https://doi.org/10.1016/j.dsr.2019.05.014>.
- Lorance, P., Latrouite, D., Séret, B., 2000. Observations of chondrichthyan fishes (sharks, rays and chimaeras) in the Bay of Biscay (North-eastern Atlantic) from submersibles. In: Séret, B., Sire, J.-Y. (Eds.), *Proceedings 3rd European Elasmobranch Association, Boulogne-Sur-Mer (France), 27-29 May, 1999*. Society France Ichthyology. & IRD, Paris, pp. 29–45, 2000.
- MarLIN, 2006. BIOTIC - Biological Traits Information Catalogue. Marine Life Information Network. Plymouth: Marine Biological Association of the United Kingdom. Available from: www.marlin.ac.uk/biotic.
- McLean, D.L., Green, M., Harvey, E.S., Williams, A., Daley, R., Graham, K.J., 2014. Comparison of baited longlines and baited underwater cameras for assessing the composition of continental slope deepwater fish assemblages off southeast Australia. *Deep-Sea Res. I* <https://doi.org/10.1016/j.dsr.2014.11.013>.
- McQuinn, I.H., Gendron, L., Himmelman, J.H., 1988. Area of attraction and effective area fished by a whelk (*Buccinum undatum*) trap under variable conditions. *Can. J. Fish. Aquat. Sci.* 45, 2054–2060.
- Palomares, M.L.D., Pauly, D. (Eds.), 2020. *SeaLifeBase. World Wide Web Electronic Publication*. www.sealifebase.org version (07/2020).
- Pingree, R.D., 1993. Flow of surface waters to the west of the British-Isles and in the Bay of Biscay. *Deep-Sea Res. Part II* 40 (1–2), 369–388. [https://doi.org/10.1016/0967-0645\(93\)90022-F](https://doi.org/10.1016/0967-0645(93)90022-F).
- Pingree, R.D., Le Cann, B., 1990. Structure strength and seasonality of the slope currents in the Bay of Biscay region. *J. Mar. Biol. Assoc. U. K.* 70 (4), 857–885.
- Prado, E., Sánchez, F., Rodríguez-Basalo, A., Altuna, A., Cobo, A., 2019. Analysis of the population structure of a gorgonian forest (*Placogorgia* sp.) using a photogrammetric 3D modeling approach at Le Danois Bank, Cantabrian Sea. *Deep Sea Res. Oceanogr. Res. Pap.* 153 <https://doi.org/10.1016/j.dsr.2019.103124>.
- Priede, I.G., Merrett, N.R., 1996. Estimation of abundance of abyssal demersal fishes: a comparison of data from trawls and baited cameras. *J. Fish. Biol.* 49, 207–216.
- Priede, I.G., Bagley, P.M., 2000. In situ studies on deep-sea demersal fishes using autonomous unmanned lander platforms. *Oceanogr. Mar. Biol. Annu. Rev.* 38, 357–392.
- Priede, I.G., Smith, K.L., Armstrong, J.D., 1990. Foraging behavior of abyssal grenadier fish: inferences from acoustic tagging and tracking in the North Pacific Ocean. *Deep Sea Research Part A. Ocean Res. Paper.* 37 (Issue 1), 81–101.
- Priede, I. G., Bagley, P.M., Smith, A., Creasey, S., Merrett, N.R., 1994. Scavenging deep demersal fishes of the Porcupine Seabight, North-east Atlantic: observations by baited camera, trap and trawl. *J. Mar. Biol. Assoc. U. K.* 74, 481–498.
- Ramsay, K., Kaiser, M.J., Moore, P.G., Hughes, R.N., 1997. Consumption of fisheries discards by benthic scavengers: utilization of energy subsidies in different marine habitats. *J. Anim. Ecol.* 66 (6), 884–896.
- Rodríguez-Basalo, A., Sánchez, F., Punzón, A., Gómez-Ballesteros, M., 2019. Updating the master management plan for el Cachucho MPA (Cantabrian Sea) using a spatial planning approach. *Continent. Shelf Res.* 184, 54–65, 2019.
- Rodríguez-Cabello, C., Sánchez, F., 2014. Is *Centrophorus squamosus* a highly migratory deep-water shark? *Deep-Sea Res. Part I* 92, 1–10.
- Rodríguez-Cabello, C., González-Pola, C., Rodríguez, A., Sánchez, F., 2018. Insights about depth distribution, occurrence and swimming behavior of *Hexanchus griseus* in the Cantabrian Sea (NE Atlantic). *Region. Stud. Marine Sci.* 23, 60–72.
- Sainte-Marie, B., Hargrave, B.T., 1987. Estimation of scavenger abundance and distance of attraction to bait. *Mar. Biol.* 94, 431–443.
- Sánchez, F., Serrano, A., Parra, S., Gómez-Ballesteros, M., Cartes, J.E., 2008. Habitat characteristics as determinant of the structure and spatial distribution of epibenthic and demersal communities of Le Danois Bank (Cantabrian Sea, N. Spain). *J. Mar. Syst.* 72, 64–86.
- Sánchez, F., Serrano, A., Gomez Ballesteros, M., 2009. Photogrammetric quantitative study of habitat and benthic communities of deep Cantabrian Sea hard grounds. *Continent. Shelf Res.* 29, 1174–1188.
- Sánchez, F., González-Pola, C., Druet, M., García-Alegre, A., Acosta, J., Cristobo, F.J., Parra, S., Ríos, P., Altuna, A., Gómez-Ballesteros, M., Muñoz-Recio, A., Rivera, J., Díaz del Río, G., 2014. Habitat characterization of deep-water coral reefs in La Gavierra canyon (Avilés canyon system, Cantabrian Sea). *Deep Sea Res.* 106, 118–140.
- Sánchez, F., Rodríguez-Basalo, A., García-Alegre, A., Gómez-Ballesteros, M., 2017. Hard-bottom bathyal habitats and keystone epibenthic species on Le Danois bank (Cantabrian Sea). *J. Sea Res.* 130, 134–153. <https://doi.org/10.1016/j.seares.2017.09.005>.
- Schobernd, Z.H., Bacheler, N.M., Conn, P.B., 2014. Examining the utility of alternative video monitoring metrics for indexing reef fish abundance. *Can. J. Fish. Aquat. Sci.* 71, 464–471.
- Sigovini, M., Keppel, E., Tagliapietra, D., 2016. Open nomenclature in the biodiversity era. *Methods Ecol. Evol.* 7, 1217–1225. <https://doi.org/10.1111/2041-210X.12594>.
- Stachowitsch, M., 1979. Movement, activity pattern, and role of a hermit crab population in a sublittoral epifaunal community. *J. Exp. Mar. Biol. Ecol.* 39, 135–150.
- Stobart, B., Díaz, D., Alvarez, F., Alonso, C., Mallol, S., Goñi, R., 2015. Performance of baited video, underwater video: does it underestimate abundance at high population densities? *PLoS One* 10 (5), e0127559. <https://doi.org/10.1371/journal.pone.0127559>.
- Stoner, A.W., Laurel, B.J., Hurst, T.P., 2008. Using a baited camera to assess relative abundance of juvenile Pacific cod: field and laboratory trials. *J. Exp. Mar. Biol. Ecol.* 354, 202–211.
- Trenkel, V.M., Lorance, P., Mahévas, S., 2004. Do visual transects provide true population density estimates for deepwater fish? *ICES (Int. Coun. Explor. Sea) J. Mar. Sci.* 61, 1050–1056.
- Tricarico, E., Gherardi, F., 2006. Shell acquisition by hermit crabs: which tactic is more efficient. *Behav. Ecol. Sociobiol.* 60, 492–500.
- Uiblein, F., Lorance, P., Latrouite, D., 2002. Variation in locomotion behaviour in northern cutthroat eel (*Synaphobranchus kaupii*) on the Bay of Biscay continental slope. *Deep Sea Res. Oceanogr. Res. Pap.* 49 (9), 1689–1703. [https://doi.org/10.1016/S0967-0637\(02\)00065-1](https://doi.org/10.1016/S0967-0637(02)00065-1).
- Uiblein, F., Lorance, P., Latrouite, D., 2003. Behaviour and habitat utilization of seven demersal fish species on the Bay of Biscay continental slope, NE Atlantic. *Mar. Ecol. Prog. Ser.* 257, 223–232.
- van Aken, H.M., 2000. The hydrography of the mid-latitude northeast Atlantic Ocean. In: *Deep Sea Research Part I: Oceanographic Research Papers*, vol. 47. Elsevier BV, pp. 789–824. [https://doi.org/10.1016/S0967-0637\(99\)00112-0](https://doi.org/10.1016/S0967-0637(99)00112-0). Issue 5.
- van Aken, H.M., 2001. The hydrography of the mid-latitude Northeast Atlantic Ocean — Part III: the subducted thermocline water mass. In: *Deep Sea Research Part I: Oceanographic Research Papers*, vol. 48. Elsevier BV, pp. 237–267. [https://doi.org/10.1016/S0967-0637\(00\)00059-5](https://doi.org/10.1016/S0967-0637(00)00059-5). Issue 1.
- van Aken, H.M., 2002. Surface currents in the Bay of Biscay as observed with drifters between 1995 and 1999. *Deep-Sea Res. Part I* 49 (6), 1071–1086. [https://doi.org/10.1016/S0967-0637\(02\)00017-1](https://doi.org/10.1016/S0967-0637(02)00017-1).
- van Rooij, D., Iglesias, J., Hernández-Molina, F.J., Ercilla, G., Gomez-Ballesteros, M., Casas, D., Llave, E., De Hauwere, A., Garcia-Gil, S., Acosta, J., Henriot, J.-P., 2010. The Le Danois contourite depositional system: Interactions between the mediterranean outflow water and the upper cantabrian slope (north Iberian margin). *Mar. Geol.* 274, 1–20. <https://doi.org/10.1016/j.margeo.2010.03.001>.
- Whitmarsh, S.K., Fairweather, P.G., Huvener, C., 2017. What is Big BRUVver up to? Methods and uses of baited underwater video. *Rev. Fish Biol. Fish.* 27, 53–73. <https://doi.org/10.1007/s1116-0-016-9450-1>.
- Willis, T.J., Millar, R.B., Babcock, R.C., 2000. Detection of spatial variability in relative density of fishes: comparison of visual census, angling, and baited underwater video. *Mar. Ecol.: Prog. Ser.* 198, 249–260.
- WoRMS Editorial Board, 2021. *World Register of Marine Species*. <https://doi.org/10.14284/170>. Available from <http://www.marinespecies.org> at VLIZ. Accessed, 2021-01-20.
- Yau, C., Collins, M.A., Bagley, P.M., Everson, I., Nolan, C.P., Priede, I.G., 2001. Estimating the abundance of Patagonian toothfish *Dissostichus eleginoides* using baited cameras: a preliminary study. *Fish. Res.* 51, 403–412.
- Yeh, J., Drazen, J.C., 2011. Baited camera observations of megafaunal scavenger ecology of the California slope. *Mar. Ecol. Prog. Ser.* 424, 145–156.